공학박사 학위논문

MAC/PHY Layer Strategies for High Efficiency WLANs

높은 효율의 무선랜을 위한 MAC/PHY 기법

2016년 8월

서울대학교 대학원

전기 · 컴퓨터공학부

유 승 민

Abstract

Along with the steady increase in mobile data traffic, wireless local area network (WLAN) technology has been developed to support heavy traffic for various mobile devices. The-state-of-art IEEE 802.11 specifications such as 802.11n and 802.11ac have focused on improving physical layer (PHY) rate by enabling multiple stream transmission via multiple-input multiple-output (MIMO) technology, wide bandwidth transmission via channel bonding, and high order modulation via 256-QAM and short guard interval. While the emerging technologies greatly increase PHY rate over 1 Gb/s, the achievable throughput is much limited due to the low reliability with high PHY rates and medium sharing among the nodes operating on the same channel. In this dissertation, we tackle three different strategies to enhance the achievable throughput in IEEE 802.11 WLANs.

Firstly, we study a cost-effective approach, namely antenna subset selection, to enhance reliability even for the high PHY rates. There are practical challenges to employ antenna subset selection in WLANs such as the lack of channel state information at the transmitter and

multiple retry chain utilization. Only few researches have addressed those practical challenges, which result in a limited employment of antenna subset selection in WLANs. We propose a practical antenna subset selection system considering those practical challenges, and evaluate the performance of the proposed system via prototype implementation and extensive experiments.

Secondly, we focus on the clear channel assessment (CCA) of IEEE 802.11 WLAN which is too conservative to exploit spatial reuse. The problem is arise due to a limitation of the current CCA mechanism. Only the received signal strength (RSS) of an ongoing transmission is used to determine the status of the medium, i.e., busy or idle. We propose a novel CCA mechanism which utilizes the information delivered in PHY header of the ongoing transmission so that it can stimulate concurrent transmissions for better spatial reuse. Through simulations, we evaluate our proposed approach and demonstrate throughput gain in various scenarios.

Lastly, we investigate transmit power and data rate control method to further exploit spatial reuse. Along with our proposed CCA mechanism, more concurrent transmissions become feasible by adapting transmit power and data rate depending on the ongoing transmission. Accordingly, we propose a joint transmit power and data rate control algorithm which operates dynamically depending on the existence of ongoing transmission. We evaluate our proposed algorithm under various scenarios through extensive simulations.

In summary, we propose three different methodologies for high efficiency WLANs, one for reliability enhancement and the other two for better spatial reuse. The operation and performance gain of each methodology are verified by testbed experiments or network level simulations.

Keywords: Wireless LAN (WiFi), antenna selection, reliability, clear channel assessment, transmit power control, rate control, high efficiency

Student Number: 2011-30245

Contents

1 Introduction **1**

1.1 Motivation 1

1.2 Overview of Existing Approaches 4

1.2.1 Practical Antenna Selection for WLAN AP . . 4

1.2.2 Protective Clear Channel Assessment 5

1.2.3 Dynamic Transmit Power and Data Rate Control 5

1.3 Main Contributions 7

1.3.1 Reliability Enhancement 7

1.3.2 Spatial Reuse Exploitation 9

1.4 Organization of the Dissertation 9

2 Practical Antenna Selection for WLAN AP **11**

2.1 Introduction 11

2.2 System Description 14

2.2.1 Characteristics of Off-the-Shelf Devices 14

2.2.2 Antenna Selection for WLAN AP 18

2.3 Measurement Studies 22

2.3.1 Throughput with Different Antenna Combinations 22
2.3.2 DL/UL Link Analysis 26
2.4 Proposed Antenna Selection Algorithm 28
2.4.1 Transmit Antenna Selection 28
2.4.2 Default Antenna Selection 36
2.5 Performance Evaluation 38
2.5.1 Performance of Proposed Transmit Antenna Selection 38
2.5.2 Performance of Proposed Default Antenna Selection 45
2.6 Summary 47

3 Protective Clear Channel Assessment 48
3.1 Introduction 48
3.2 Background and Motivation 50
3.2.1 Ideal Operation of CCA 50
3.2.2 IEEE 802.11 Frame Format and CCA Method 52
3.2.3 Physical Layer Header Utilization for CCA . . 54
3.3 Protective Clear Channel Assessment 55
3.3.1 Signal Quality Table 56
3.3.2 Feasibility Check of Spatial Reuse 57
3.3.3 Consideration of Link Asymmetry 58
3.4 Performance Evaluation 60

3.5 Summary 64

4 Dynamic Transmit Power and Data Rate Control 66

4.1 Introduction 66

4.2 Transmit Power and Rate Control for Spatial Reuse 68

4.2.1 RTS-CTS Based 69

4.2.2 Feedback Based 70

4.2.3 Limitations of existing approach 71

4.3 Dynamic Transmit Power and Rate Control 72

4.3.1 Information Gathering 73

4.3.2 Dynamic TPC & RA 76

4.3.3 Normal TPC & RA 77

4.3.4 DCF Throughput Analysis 78

4.3.5 Multi-cell Consideration 85

4.4 Performance Evaluation 86

4.5 Summary 91

5 Conclusion 93

5.1 Research Contributions 93

5.2 Future Research Directions 95

List of Tables

2.1 AP configuration. 24

2.2 Measurement result summary. 27

2.3 Correlation coefficients (r) and p-values (p). 27

2.4 Summary of transmit antenna throughput. 44

2.5 Summary of default antenna performance. 47

3.1 An example of T_2's Signal Quality Table. 56

4.1 An example of T_2's Signal Quality Table. 73

4.2 An example of back-off counter change. 79

4.3 Summary of IEEE 802.11 parameters. 81

4.4 Simulation parameters for residential building topology. 87

4.5 Throughput result with the residential building topology. 89

List of Figures

1.1 Data rate with different WLAN standards. 3

1.2 Coverage of different data rates. 3

2.1 Transmission parameters for multiple retry chains. . . 15

2.2 Antenna selection system example of infrastructure-based WLAN. 16

2.3 Transient throughput according to antenna combinations at three different positions. 23

2.4 Office environment for measurement. 24

2.5 Average fade duration of selection combining. 32

2.6 Temporal throughput change with transmit antenna selection: Single station case. 39

2.7 Temporal throughput change with transmit antenna selection: Multiple station case. 40

2.8 Empirical CDF of throughput with three different speeds. 43

2.9 Temporal performance of the worst station with MiDAS in static channel environments. 46

3.1 CCA result depending on the possibility of capture effect. 50
3.2 IEEE 802.11 physical layer frame format. 52
3.3 Simulation topology for two overlapping cells. 60
3.4 Performance of Legacy (−82 dBm). 61
3.5 Performance of Legacy (−62 dBm). 61
3.6 Performance of ProCCA. 61
3.7 Performance with two-tier hexagonal cell topology. . . 63

4.1 Overall structure of DynamicReuse. 70
4.2 RSS of previous packet feedback after second capture. 75
4.3 DCF throughput with lowered data rate. 83
4.4 Multicell example of DynamicReuse. 85
4.5 Simulation topology for two overlapping cells. 86
4.6 Residential building topology for high density environment. 87
4.7 Performance of Legacy (−82 dBm). 88
4.8 Performance of ProCCA. 88
4.9 Performance of DynamicReuse. 88
4.10 Empirical CDF of throughput with the residential building topology. 90

Chapter 1

Introduction

1.1 Motivation

Wireless local area network (WLAN) technology has become an indispensable part of our daily lives as a dominant carrier of wireless data traffic. The worldwide chipset shipment and wireless data traffic of WLAN have increased steadily, and further increase is forecasted.

To support heavy data traffic, IEEE 802.11 specifications have been developed primarily focused on theoretical peak throughput in a single basic service set (BSS)[1] environment. The-state-of-art IEEE 802.11 specifications such as 802.11n and 802.11ac adopt multiple stream transmission via multiple-input multiple-output (MIMO) technology, wide bandwidth transmission via channel bonding, and high order modulation via 256-QAM and short guard interval to enhance

[1] A BSS is composed of an access point and a number of associated stations.

the peak throughput. While the emerging technologies greatly increase PHY rate over 1 Gb/s as shown in Fig. 1.1, the achievable throughput is much limited in the real world. It is due mainly to the low reliability with the high data rates and medium sharing among the nodes operating on the same channel:

1. Reliability issue: The reliability of a data rate decreases as the data rate increases, which result in the coverage reduction as shown in Fig. 1.2. The coverage of highest data rate is even less than 5 m, i.e., we should be in 5 m from an access point (AP) to exploit the highest data rate. To exploit the high data rates without such limitation, the reliability should be enhanced.

2. Medium sharing issue: When multiple BSSs operate on the same channel in WLANs, the medium (channel) is shared among the OBSSs, which is a very practical scenario in the real world. With the heavy data traffic, the theoretical peak throughput of a single BSS is inversely proportional to the number of BSSs, which result in the low throughput of high density WLANs. Meanwhile, exploiting spatial reuse, by enabling concurrent transmissions, the achievable throughput can be enhanced.

In this dissertation, accordingly, we tackle three different strategies to enhance the achievable throughput in IEEE 802.11 WLANs, practical antenna selection of WLAN AP (Chapter 2) for reliability enhancement, and a novel clear channel assessment (CCA) mechanism

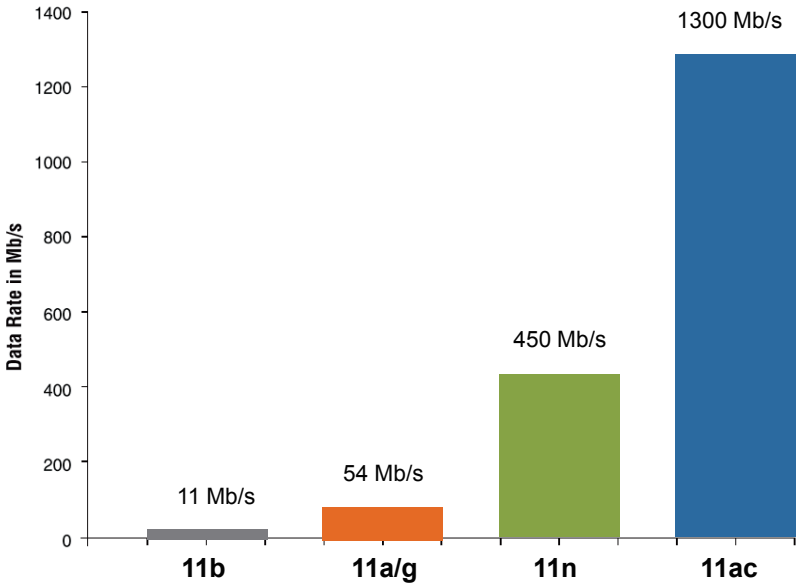

Figure 1.1: Data rate with different WLAN standards.

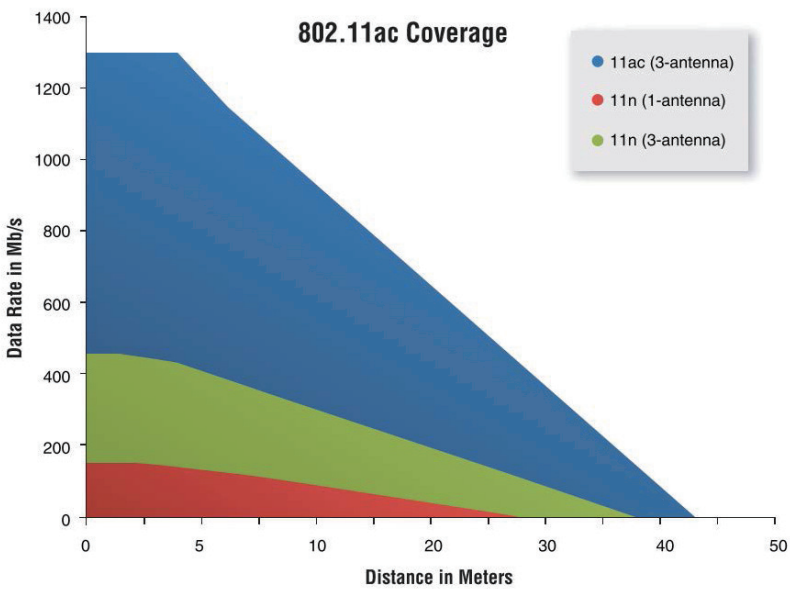

Figure 1.2: Coverage of different data rates.

(Chapter 3) and dynamic transmit power and rate control mechanism (Chapter 4) for the better spatial reuse.

1.2 Overview of Existing Approaches

1.2.1 Practical Antenna Selection for WLAN AP

There has been extensive research in antenna subset selection algorithms [1, 2, 3, 4, 5, 6, 7]. The authors in [1, 2, 3, 4] utilize instantaneous channel state information (CSI) to select an optimal antenna subset. Similarly, statistical CSI is utilized for the antenna subset selection in [5, 6, 7]. However, off-the-shelf WLAN devices do not implement CSI feedback functionality due to its significant overhead, thus limiting the applications of the proposed schemes in [1, 2, 3, 4, 5, 6, 7]. To the best of our knowledge, there is no research paper in the literature that proposes antenna subset selection algorithm without utilizing CSI.

Meanwhile, a couple of patents deal with antenna subset selection system without using CSI. In [8], an antenna subset is selected using a trial-and-error approach, i.e., a single antenna subset is selected and used until a transmission failure occurs. In [9], an optimal antenna subset is determined based on statistical information. The information is obtained by probing, i.e., periodically transmitting frames using different antenna subsets. Although the patents describe the example procedures, detailed algorithms and performance evaluations are not

presented due to the nature of patent.

1.2.2 Protective Clear Channel Assessment

Since the CCA highly affects the network capacity via exploiting spatial reuse, there have been many studies on controlling CST for efficient medium sharing. Analytic approaches proposed in [10, 11] focus on addressing the hidden terminal problem, which results in a conservative CST to eliminate all possible hidden transmitters in the entire range. Such a conservative CST obstructs concurrent transmissions even when they are possible, i.e., exposed terminal problem. On the other hand, heuristic approaches based on the frame error rate yield a less conservative CST by heuristically considering only some possible hidden transmitters [12, 13].

However, the current CCA method has an inherent limitation in that it utilizes only the received signal strength (RSS) of an incoming frame to determine the availability of the medium. As a result, a carrier sensing node cannot be aware of whether it can transmit along with an ongoing transmission, i.e., a concurrent transmission, which is possible when its transmission will not harm the ongoing transmission from another cell.

1.2.3 Dynamic Transmit Power and Data Rate Control

There have been many researches of transmission power control for spatial reuse. The researches can be classified into two categories,

namely RTS-CTS based approach and feedback based approach.

Several papers try to reduce transmit power of data transmissions while avoiding the collision from hidden nodes by differentiating the power of RTS-CTS and data-ACK transmissions. In [14], RTS-CTS packets are transmitted with the maximum power, and the transmit powers of data-ACK packets are reduced accordingly to avoid hidden collisions. The authors in [15] extend the work in [14], and they also control the transmit power of RTS/CST packets considering the transmission range and interfering range to avoid hidden collisions but enhance spatial reuse. However, this approach is conservative to enabling concurrent transmissions due to RTS-CTS packets are exchanged with high power, and the nodes consider all the possible interfering nodes in the interfering range which are not always exist.

To exploit spatial reuse by enabling concurrent transmissions without the loss from hidden terminals, the feedback based approach tries to find interference levels and allowable interference levels among the nodes operating in the same medium [16, 17, 18]. The allowable interference level of a receiver node is fed back to the corresponding transmitter node, e.g., via an out-of-band channel in [16], a separate control channel in [17], and RTS/CTS exchange at access window in [18], and the transmitter node decides it's proper transmit power. When the transmitter node decodes the transmit power, it considers all the possible future interferers in the medium because all the interferer can corrupt the transmission, and the transmitter does not

know who will corrupt the transmission in presence.

Existing data rate control focus on finding appropriate data rate based on the channel condition, thus there are a limited number of researches on data rate control for spatial reuse [19, 20]. In [20], the authors lower the data rate to fully exploit the medium even if there are throughput reduction with the lowered rate. The authors in [19] also lower the data rate to tolerate interference even though throughput is possible to decrease. The main limitation of existing data rate control is the throughput decrease with the lowered data rate.

1.3 Main Contributions

The main objective of this dissertation is to provide high efficient MAC and PHY layer algorithms to exploit the high data rates of emerging IEEE 802.11 WLAN technologies. They can be classified in two categories, namely reliability enhancement and spatial reuse exploitation. More into detail, the research contributions of the dissertation are summarized as follows.

1.3.1 Reliability Enhancement

Since there a well-known trade-off between spatial multiplexing gain and spatial diversity gain, reliability cannot be enhanced via MIMO for high data rates even though the higher data rate is more unre-

liable. Antenna subset selection is a cost effective way to achieve diversity gain without such limitations. By employing more antennas than RF chains and adaptively connecting each RF chain to one of the available antennas, diversity gain can be obtained without loss of multiplexing gain. However, there are some practical challenges for antenna subset selection of 802.11 WLAN device, and no research paper has been provided proper selection algorithm considering the practical challenge.

We proposed antenna selection algorithm considering the practical issues, and the proposed algorithm has three different main advantages. The first advantage is practicality. The proposed algorithms are designed to be applicable to commercial WLAN chipsets, which utilize multiple retry chains for a packet transmission. In addition, only currently available information in WLANs, e.g., frame success ratio (FSR), is used. The practicality is proved by a prototype implementation of the proposed algorithms in a commercial AP. The second advantage is robustness. The best and the second best antenna subsets are used alternatively to achieve diversity gain, thus reducing the occurrence of consecutive transmission failures. The last advantage is self-regulation. The frequency of probing is automatically adjusted depending on channel condition, i.e., more probing for bad channel and less probing for good channel, thus minimizing probing overhead.

1.3.2 Spatial Reuse Exploitation

In densely deployed network, which has many AP devices and corresponding client stations operating on the same channel, the throughput is greatly degraded even thought their operational data rates are high enough since they should share the medium, i.e., the operating channel. Spatial reuse can enhance the throughput via stimulating more concurrent transmissions. In 802.11 WLANs, the degree of spatial reuse is determined by CCA, transmit power, and data rate. Firstly, we proposed a novel CCA mechanism which utilizes PHY layer header information and determines the state of medium (busy/idle). By utilizing the header information, the proposed mechanism can examine the possibility of concurrent transmission with the ongoing transmission, so that it can exploit proper spatial reuse if it is possible. Secondly, we proposed a dynamic transmit power and data rate control algorithm which adapt the transmit power and data rate depending on the ongoing transmission, which significantly enhances spatial reuse by enable more concurrent transmissions, thus result in great improvement of network performance.

1.4 Organization of the Dissertation

Chapter 2 presents the practical antenna selection policies to enhance reliability of multiple antenna AP devices. We first introduce the practical challenges of commercial AP devices for antenna selection

algorithms and achievable throughput enhancement with antenna selection via measurement study using off-the-shelf devices. We proposed practical antenna selection algorithms for transmission and reception of AP devices, and the performance is evaluated via extensive experiments with off-the shelf devices.

In Chapter 3, we present the novel CCA method to enhance network-wise throughput of high density WLANs. Specifically, the proposed CCA utilizes physical layer header information to assure the success of concurrent transmission including ongoing transmission and corresponding new transmission, so that concurrent transmissions are more stimulated depending on the ongoing transmission.

Chapter 4 presents our proposed transmit power and data rate control algorithms to exploit spatial reuse. By theoretical analysis, we show that our proposed approach which dynamically adapts the transmit power and data rate depending on ongoing transmission can enhance the throughput as optimal without loss of fairness. The throughput performance is evaluated via ns-3 simulation.

Finally, Chapter 5 concludes the dissertation with the summary of contributions and discussion on the future work.

Chapter 2

Practical Antenna Selection for WLAN AP

2.1 Introduction

Multiple-input multiple-output (MIMO) technology is an indispensable part of wireless local area networks (WLANs) because of increased data rate by spatial multiplexing and reliability enhancement by spatial diversity. Unfortunately, there is a trade-off between spatial multiplexing and diversity, i.e., maximum spatial multiplexing gain is achievable with the sacrifice of diversity gain, and vice versa [21]. Therefore, extra antennas are needed to increase diversity gain along with a certain degree of multiplexing gain. However, there are two main limitations in increasing the number of antennas, namely, the hardware costs of radio frequency (RF) chains (including RF power

amplifier and analog-to-digital/digital-to-analog converter, etc.) for each antenna and the computational complexity for signal encoding and decoding process.

Antenna subset selection is a cost effective way to achieve diversity gain without such limitations. By employing more antennas than RF chains and adaptively connecting each RF chain to one of the available antennas, diversity gain can be obtained without loss of multiplexing gain. It was proved that such antenna subset selection retains the same degree of diversity compared with the full-complexity system, i.e., the system with the same numbers of antennas and RF chains [22].

There has been extensive research in antenna subset selection algorithms [1, 2, 3, 4, 5, 6, 7]. The authors in [1, 2, 3, 4] utilize instantaneous channel state information (CSI) to select an optimal antenna subset. Similarly, statistical CSI is utilized for the antenna subset selection in [5, 6, 7]. However, off-the-shelf WLAN devices do not implement CSI feedback functionality due to its significant overhead, thus limiting the applications of the proposed schemes in [1, 2, 3, 4, 5, 6, 7]. To the best of our knowledge, there is no research paper in the literature that proposes antenna subset selection algorithm without utilizing CSI.

Meanwhile, a couple of patents deal with antenna subset selection system without using CSI. In [8], an antenna subset is selected using a trial-and-error approach, i.e., a single antenna subset is selected and used until a transmission failure occurs. In [9], an optimal antenna

subset is determined based on statistical information. The information is obtained by probing, i.e., periodically transmitting frames using different antenna subsets. Although the patents describe the example procedures, detailed algorithms and performance evaluations are not presented due to the nature of patent.

The main purpose of this chapter is to develop a practical antenna subset selection method for off-the-shelf devices without any modification or additional requirement of IEEE 802.11 standard and WLAN chipsets. We propose antenna subset selection algorithms of access point (AP) (a) for unicast transmission and (b) for multicast transmission and reception. Compared with the existing schemes in the literature, the main advantages of our proposed algorithms are:

1. Practicality: The proposed algorithms are designed to be applicable to commercial WLAN chipsets, which utilize multiple retry chains for a packet transmission. In addition, only currently available information in WLANs, e.g., frame success ratio (FSR), is used. The practicality is proved by a prototype implementation of the proposed algorithms in a commercial AP.

2. Robustness: The best and the second best antenna subsets are used alternatively to achieve diversity gain, thus reducing the occurrence of consecutive transmission failures.

3. Self-regulation: The frequency of probing is automatically adjusted depending on channel condition, i.e., more probing for

bad channel and less probing for good channel, thus minimizing probing overhead.

The rest of the chapter is organized as follows: Section 2.2 describes the current status of infrastructure-based WLAN. We demonstrate the potential for network performance improvement via antenna selection through measurements in Section 2.3. Then, we propose practical antenna selection algorithms for transmission and reception of AP in Section 2.4, and then evaluate the performance of the algorithms through an extensive measurement study in Section 2.5. Finally, we draw the summary in Section 2.6.

2.2 System Description

In this section, we first describe the characteristics of off-the-shelf devices, which constitute infrastructure-based WLAN. Then, we describe the antenna selection system considering the characteristics and limitations of off-the-shelf devices.

2.2.1 Characteristics of Off-the-Shelf Devices

There are four characteristics of off-the-shelf devices which should be considered for practical antenna selection systems.

Multiple retry chains: Most commercial WLAN devices use multiple retry chains. For example, Qualcomm Atheros (QCA) WLAN chipsets use four different retry chains. A transmission descriptor is

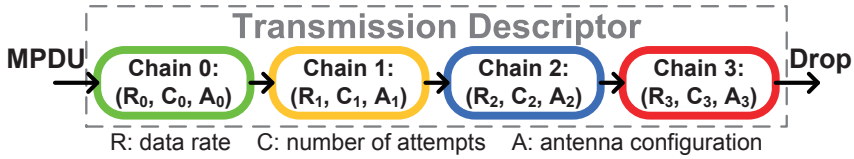

Figure 2.1: Transmission parameters for multiple retry chains.

configured for each MAC protocol data unit (MPDU) and describes the transmission parameters of each retry chain, i.e., the data rate (r_i), the maximum number of tries (n_i), and the antenna configuration (c_i) for retry chain i, as shown in Fig. 2.1. The first transmission of an MPDU uses data rate, r_0, and antenna configuration, c_0. If the transmitter does not receive the corresponding acknowledgement (ACK) for the first transmission, the MPDU is retransmitted up to $(n_0 - 1)$ times with r_0 and c_0. If all n_0 (re)transmissions fail, then r_1 and c_1 are used for the next n_1 retransmissions, and r_2/c_2 and r_3/c_3 are sequentially used until the packet is successfully transmitted or dropped.[1]

Spatial expansion: Data streams can be expanded via matrix multiplication to produce the input to all the RF chains, namely spatial expansion. For instance, matrix $D = \frac{1}{\sqrt{3}}[111]^T$ is used to map a single data stream to three RF chains, i.e., it is replicated and transmitted through three RF chains with reduced power. With the spatial expansion, the AP can take an advantage related to power amplifier. Since the total power is divided into the employed RF chains,

[1]If all the retransmission attempts fail, the MPDU will be dropped.

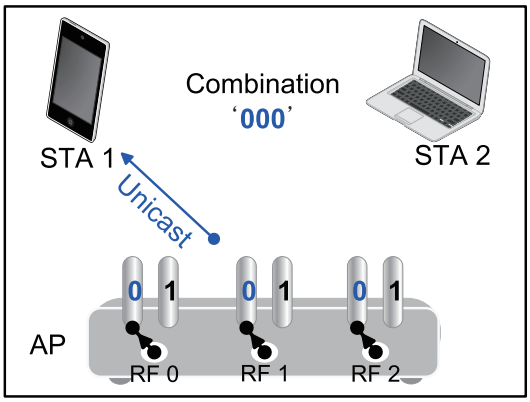

(a) Unicast to station 1

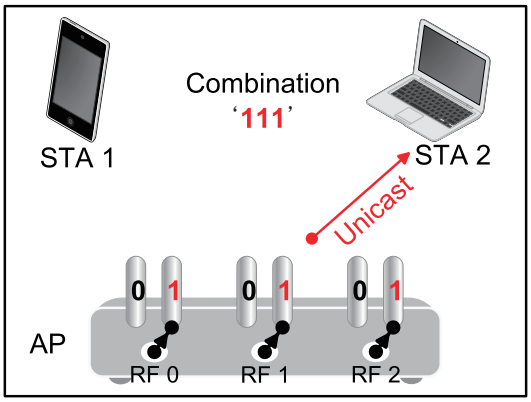

(b) Unicast to station 2

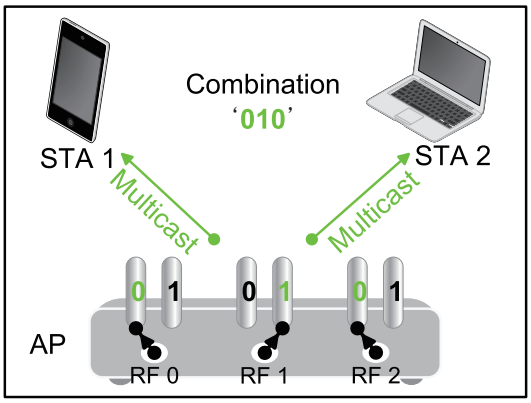

(c) Multicast

Figure 2.2: Antenna selection system example of infrastructure-based WLAN.

the power amplifier of each RF chain can share the burden for the maximum power, thus allowing to use cheaper power amplifier. Accordingly, many WLAN chipsets including QCA chipsets use spatial expansion by default. In this work, thus, we assume that the AP always utilizes all the RF chains regardless of the number of data streams.

Antenna subset selection: QCA chipsets adopt antenna subset selection using RF switches which connect antennas to RF chains according to the antenna configuration in the transmission descriptor. Different from general antenna subset selection, specifically, one of the antennas confined to an RF chain is connected to the corresponding RF chain. As we assume spatial expansion, therefore, an antenna subset can be denoted by a combination, which consists of the antennas each connected to the corresponding RF chain, and we use the term, antenna combination, hereafter. In this paper, furthermore, antenna selection means antenna combination selection for the RF chains.

***No CSI feedback*:** There are two methods for obtaining downlink (DL) CSI at an AP, namely, implicit feedback and explicit feedback [23]. The former utilizes the channel reciprocity, so the AP estimates DL CSI from uplink (UL) signal. However, the RF chains of an AP and its client station are different from each other, thus contaminating the CSI estimation. Thus, a calibration process is defined in IEEE 802.11 standard to remove the contamination from the RF chain mismatch [23]. In the latter, a station measures DL CSI and

feeds it back to the AP. However, the CSI feedback feature is not implemented in any commercial WLAN chipsets due to the prohibitive feedback overhead versus a benefit. Without the CSI feedback, even the calibration for the implicit method is not feasible. Therefore, the AP can obtain the CSI neither by the explicit feedback nor the implicit feedback.

Instead of CSI feedback, IEEE 802.11ac adopts feedback of compressed beamfoming matrix along with per-stream SNR for multi-user MIMO operation [24]. DL CSI is, however, still not available at AP. Furthermore, even if DL CSI becomes available, learning CSI of all possible combinations will bring excessive signaling overhead.

In summary, an antenna combination can be configured for each retry chain of each MPDU by the transmission descriptor. Different from the previous antenna selection algorithms in the literature, CSI cannot be used for practical antenna selection in WLANs.

2.2.2 Antenna Selection for WLAN AP

Problem statement: For a practical antenna selection system with off-the-shelf devices, we only consider antenna combination selection of AP side in infrastructure-based WLAN.[2] We assume that the number of RF chains is M and each RF chain has L antennas, and hence, there are total L^M combinations, one of which can be selected for transmission/reception. For the ease of our explanations, we consider

[2]Typically, APs have more RF chains than other WLAN devices.

the case of M=3 and L=2 as shown in Fig. 2.2, so there are 8 possible combinations.

Antenna selection of AP can be classified into two cases, namely, transmit antenna selection and default antenna selection. Transmit antenna is for unicast transmission which aims to a specific target station as shown in Figs. 2.2(a) and 2.2(b), while default antenna is used for the reception of UL frames[3] or the transmission destined to multiple stations, e.g., multicast transmission and beacon transmission, as shown in Fig. 2.2(c). Therefore, default antenna combination should be selected considering all the associated stations of an AP.

Without CSI feedback, only two types of information are available for antenna selection, namely, frame success ratio (FSR) via ACK and received signal strength indicator (RSSI) of UL frames. The antenna selection should be performed in an open-loop manner using the information. However, the RSSI of UL is significantly different from that of DL due to the asymmetry between the RF chains of AP and stations as well as receiver combining methods, as detailed in Section 2.3. For this reason, the RSSI of UL cannot be utilized for antenna selection, and AP should select transmit/default antenna based on the frame success statistics.

Mathematical description: As we assume spatial expansion, data symbol received at a station, when AP transmits a single data

[3]Intuitively, the selected transmit antenna combination is used for the corresponding ACK frame reception while the default antenna combination is used for any other reception since AP does not know the target station in advance of reception.

stream through antenna combination $c = (a_1, a_2, ..., a_M)$, can be expressed as:

$$y_{\mathrm{c}} = y_{(a_1,a_2,...,a_M)} = hx + n = \sum_{i=1}^{M} g_{i,a_i} h_{i,a_i} x + n, \tag{2.1}$$

where a_i is the selected antenna index for RF chain i ($a_i \in \{0, 1, ..., L-1\}$), and n is additive white Gaussian noise (AWGN) with the variance equal to N_0. g_{i,a_i} and h_{i,a_i} are the antenna gain and fading coefficient of RF chain i with a_i, respectively. We assume independent Rayleigh fading channel for each antenna.[4] Therefore, h_{i,a_i} is a complex Gaussian random variable with zero mean and unit variance, and there is no correlation among different antennas. It should be noted that the superposed channel h is also a complex Gaussian random variable with zero mean and variance, equal to $\sum_i g_{i,a_i}^2$, thus making h a Rayleigh fading channel.

The signal-to-noise ratio (SNR) at the receiving station, i.e., SNR of DL signal, is given by

$$SNR_{\mathrm{DL}} = P_{\mathrm{s}} \left|\sum\nolimits_i g_{i,a_i} h_{i,a_i}\right|^2 / N_0, \tag{2.2}$$

where P_{s} is the average power of the data symbol (x) at the receiving station.

AP selects a default antenna combination to receive UL signal, and

[4]This assumption is only for clearer mathematical description, while our antenna selection algorithms do not rely on this assumption.

the received data symbol at the AP can be also expressed as (2.1). Unlike the DL signal, however, the AP can conduct a receiver combining such as maximal ratio combining (MRC) or equal gain combining (EGC) to achieve diversity gain. In this paper, we assume MRC is used, so the SNR of UL signal at the AP is given as

$$SNR_{\mathrm{UL}} = P_{\mathrm{s}} \sum\nolimits_i |g_{i,a_i} h_{i,a_i}|^2 / N_0. \tag{2.3}$$

The antenna gain, g_{i,a_i}, varies depending on the target station and its position since different antennas have different radiation patterns. Therefore, by choosing the antenna combination which consists of the antennas giving maximum gain for each RF chain i as

$$c_{\max} \triangleq (a_{\max,1}, ..., a_{\max,M}), \tag{2.4}$$

where $a_{\max,i} = \arg\max_{a_{j,i}} g_{i,a_{j,i}}$, the average SNRs of both UL and DL signals are maximized. Meanwhile, DL SNR is more vulnerable to fading than UL SNR as shown in (2.2) and (2.3). It is because receiver combining of UL helps make constructive superposition of received symbol while DL cannot avoid destructive superposition. Although we only derive (2.1)–(2.3) for single stream, it is obvious that $c_{\max}$ also gives the maximum average SNR for multiple streams.

In this paper, the antenna selection is aimed at finding $c_{\max}$ which maximizes throughput in a long-term average sense. The long-term average throughput does not depend on the instantaneous fading co-

efficient (h_{i,a_i}), because the mean of h_{i,a_i} is one for all a_i's. The instantaneous CSI, therefore, is not essential for the antenna selection.

2.3 Measurement Studies

This section demonstrates the potential for performance improvement by antenna selection and investigates several considerations for designing antenna selection algorithms.

2.3.1 Throughput with Different Antenna Combinations

We first measure throughput according to antenna combination to gauge the performance gain from the antenna selection.

The measurements are carried out in an office environment shown in Fig. 2.4. Samsung WEA303 AP and Samsung Galaxy S3 smartphones are used. WEA303 supports 802.11n MIMO up to 3 streams with 3 RF chains and 2 antennas for each RF chain [25] while Samsung Galaxy S3 supports 802.11n single stream only [26]. The station is placed at 6 different positions as shown in Fig. 2.4, where the position index represents the ranking of average RSSI at the position. Using IxChariot 7.3 [27], DL UDP traffic with 1460 bytes payload size is generated, and throughput is measured for 10 seconds. We repeat this measurement 8 times by switching antenna combination to compare the throughput according to the 8 different antenna combi-

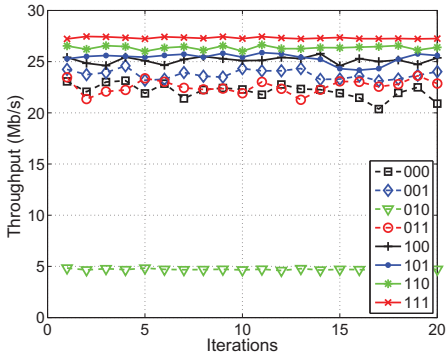

(a) Position 5

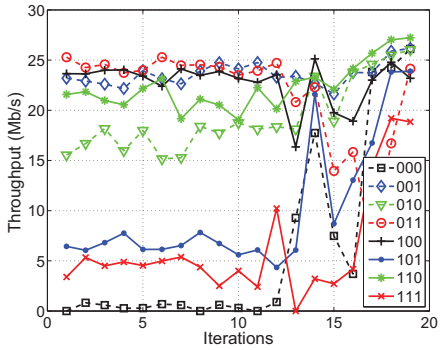

(b) Position 6

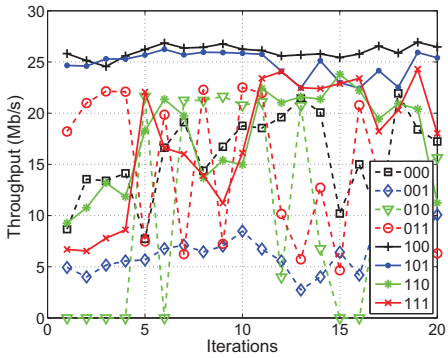

(c) Position 3

Figure 2.3: Transient throughput according to antenna combinations at three different positions.

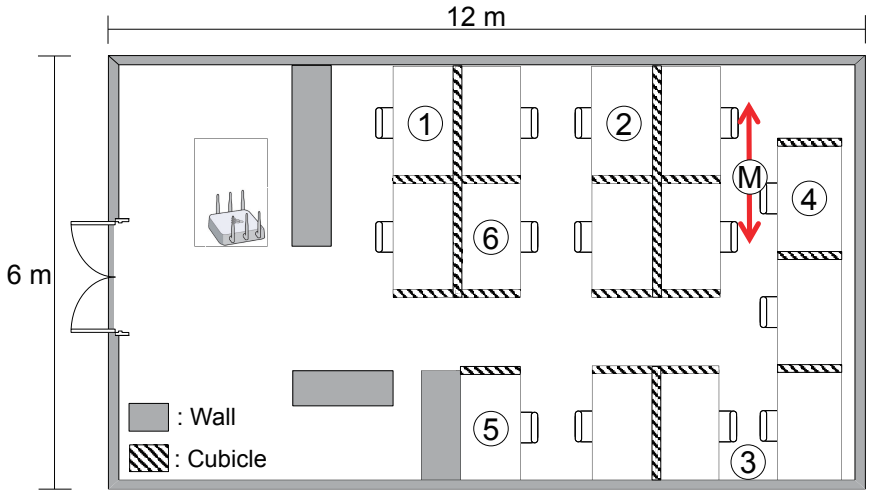

Figure 2.4: Office environment for measurement.

Table 2.1: AP configuration.

Channel	Ch. 48 (5,240 MHz)
Data rates	MCS 0–7
Tx power	17 dBm
Frame aggregation	Disabled
Guard interval	Regular (0.8 μs)

nations (L^M=2^3=8). One *iteration* consists of these 8 measurements, and 20 iterations are carried out at each position. During the measurement, no or just a single person is sitting in the office to make a stationary environment, and we maintain this condition for all the measurements throughout this paper. The AP is configured to use channel 48, which is clean without any interference, and detailed configuration is described in Table 2.1.

Fig. 2.3 shows the average throughput for each iteration at three

different positions. The measurements for 8 different antenna combinations in the same iteration are carried out at almost same time, and hence, can be construed as a transient performance according to the combination. Fig. 2.3(a) shows the result for position 5, where the channel for all antenna combinations is stable. Therefore, the throughput for each antenna combination does not fluctuate much according to the iterations. At the position, antenna combination '111' achieves the highest throughput while combination '010' obtains the lowest throughput regardless of the iterations. This shows that selecting a proper antenna combination can significantly enhance throughput performance at certain positions. On the other hand, Figs. 2.3(b) and 2.3(c) presenting the results for positions 6 and 3 show temporal variation of throughput. At position 6, for instance, the throughput of antenna combination '101' varies from 5 Mb/s to 24 Mb/s over iterations. Whether the channel is stable or not, there exists the best antenna combination at an iteration and it depends on the station's position, e.g., '111' at position 5 and '100' at position 3 (except iteration 3). Furthermore, the best combination of previous iteration can show degraded throughput compared with other combinations due to fading, e.g., the throughput of '011' at position 6 rapidly decreases after iteration 12. It is because each antenna combination could experience fading due to destructive superposition in DL as described in Section 2.2, and there is no exception for the best combination.

The throughputs and RSSIs measured at 6 positions are summa-

rized in Table 2.2. Avg. and std. represent the average and standard deviation of performances out of 8 antenna combinations, respectively. Last row shows the throughput gain of the best antenna combination over the average throughput of 8 antenna combinations. According to the table, the throughput gain from antenna selection highly depends on the station's position. At positions 3, 5, and 6, the gain is above 20% while the relatively negligible gain is observed at the other positions. By comparing position 1 with 5, and position 3 with 4, we observe that the positions with high throughput gain are characterized by low average RSSI and high standard deviation of RSSI. This shows that, at a certain position, a significant performance gain can be achieved by selecting a proper antenna combination.

2.3.2 DL/UL Link Analysis

Next, we study the relationship between UL and DL based on measurement results. We carry out a similar measurement as in Section 2.3.1, but with different station positions. At each position, DL and UL UDP traffic are alternatively generated for 10 seconds. Similarly, 10 iterations are conducted at each position and the measurement result is summarized in Table 2.3. In the top side, Pearson's correlation coefficients r and p-values[5] from 80 pairs, i.e., 8 antenna combinations $\times$ 10 iterations, of (UL RSSI, DL throughput) are displayed for each position. In terms of every position, r is observed to

[5] p-value represents the reliability of the obtained correlation, and p-value under 0.01 means significantly high reliability.

Table 2.2: Measurement result summary.

Position		1	2	3	4	5	6
RSSI (dBm)	Avg.	−65	−68	−68	−68	−68	−70
	Std.	3.22	3.62	9.67	2.56	3.25	6.65
Throughput (Mb/s)	Avg.	26.7	24.9	17.4	26.6	22.2	17.6
	Std.	0.38	0.31	3.97	0.45	0.37	5.22
	Gain	7%	8%	60%	4%	23%	52%

Table 2.3: Correlation coefficients (r) and p-values (p).

		1	2	3	4	5	Avg.
UL RSSI	r	−0.33	−0.34	−0.16	+0.27	−0.15	−0.14
DL THR	p	0.46	0.46	0.51	0.51	0.51	0.49
DL THR	r	+0.96	+0.94	+0.77	+0.78	+0.99	+0.89
UL THR	p	< 0.01	< 0.01	0.05	0.08	< 0.01	0.03

have the value close to zero rather than one as well as the high level of p. This indicates we cannot say there is any correlation between UL RSSI and DL throughput. UL RSSI, therefore, is not a proper metric for transmit antenna selection.

On the other hand, there exists a distinct correlation between DL throughput and UL throughput as displayed in the bottom side, i.e., r close to 1 and p under 0.1. This result demonstrates that the antenna combination with good DL performance is likely to work well for UL as expected by the mathematical analysis in Section 2.2. That is, according to (2.2) and (2.3), although the instantaneous RSSI values of DL and UL (RSSI=SNR$\cdot N_0$) can be different, the combination $c_{\max}$ in (2.4) gives the maximum average SNR for both DL and UL, thus

giving the throughput correlation between DL and UL.

2.4 Proposed Antenna Selection Algorithm

In this section, we propose antenna selection algorithms to determine AP's transmit and default antenna combinations. As shown in Section 2.3, UL RSSI is not a proper metric to be used for antenna selection. Therefore, the proposed algorithms utilize only the frame success statistics, gathered based on ACK reception.

2.4.1 Transmit Antenna Selection

The key observations in Section 2.3 for transmit antenna selection are twofold. First, there exists difference of performances between antenna combinations, and the best one could vary depending on the station (position). Second, as the wireless channel fluctuates over time, even the best combination can experience fading, thus resulting in considerable throughput degradation.

Best1Probe: Focusing on the first observation, we establish a baseline algorithm which finds the best antenna combination using frame success ratio (FSR) statistics.[6] The antenna selection method in [9] performs probing, when it is not a retransmission, to gather statistics of antenna configurations which are not being currently used, and updates the best antenna configuration based on FSR. We con-

[6] FSR is the ratio of the number of successful transmissions, determined by ACK reception, to the total number of transmissions including retransmissions.

linesnumbered 1 Best1Probe

```
Set T_interval                                  ▷ set time interval for decision
while transmission do
    timer ← 0
    P_0(c_best), P_0(c_probe) ← 0               ▷ init. FSR of retry chain 0
    while timer < T_interval do
        if Probing then ▷ 10% of packets are utilized for probing
            S_probe ← (c_probe, c_best, c_best, c_best)   ▷ antenna series for probing
            Use S_probe
        else
            S_best ← (c_best, c_best, c_best, c_best)     ▷ antenna series for normal
            Use S_best
        end if
        Update P_0(c_best) and P_0(c_probe)
    end while
    c_best ← arg max_{c_i ∈ {c_best, c_probe}} P_0(c_i)
    Pick new c_probe randomly
end while
```

struct the baseline algorithm following the basic procedure in [9], and referring to Minstrel rate control algorithm [28] for the detailed operation.[7]

The procedure of the baseline algorithm, called Best1Probe, is described in Algorithm 1. Basically, FSR of the currently used antenna combination, i.e., the best combination (c_{best}), and FSR of probed antenna combination (c_{probe}) are gathered during a time interval (T_{interval}). At the end of T_{interval}, the combination which has higher FSR is determined as c_{best} for the next T_{interval}. Every T_{interval},

[7]Minstrel is a widely-used rate control algorithm which utilizes FSR to find the best rate, and performs probing to get statistical information of unused rates.

c_{probe} is changed randomly or sequentially to find the best antenna combination among all possible combinations. Data rates of retry chains can be different from each other, so FSRs of different antenna combinations should be compared not across the retry chains but only in the same retry chain. Therefore, FSRs of the two combinations are measured and compared only for retry chain 0 which is mostly tried with a proper rate control.

As explained in Section 2.2, antenna combinations for four retry chains of a packet can be configured by transmission descriptor. We define antenna combination series, S, as the configured four antenna combinations, (c_0, c_1, c_2, c_3). The baseline algorithm finds only the best antenna combination, so S is configured to $(c_{\text{best}}, c_{\text{best}}, c_{\text{best}}, c_{\text{best}})$ for normal case and $(c_{\text{probe}}, c_{\text{best}}, c_{\text{best}}, c_{\text{best}})$ for probing.

Best2Probe: We should be reminded of the second observation that the best combination can experience fading since DL cannot obtain diversity gain by receiver combining. In other words, using only the best antenna combination for transmission can be vulnerable to fading. Obviously, one way to obtain diversity gain for DL is to use different antenna combinations by turns.

To investigate the diversity gain from using different antenna combinations alternatively, we exploit a well-known metric to assess diversity techniques, average fade duration (AFD), which quantifies how long a channel gain stays below a certain fading threshold. AFD of the case when N antenna combinations are alternatively used (AFD_{au})

approximates AFD of selection combining (AFD_{sc}), where selection combining selects the antenna which has the maximum channel gain among N candidates, and the relation can be expressed as

$$AFD_{\text{au}} \leq AFD_{\text{sc}} + N\triangle t, \tag{2.5}$$

where $\triangle t$ is the time interval of changing combinations. The inequality holds because the antenna combination which has the maximum channel gain will be used within $N\triangle t$ for the alternative usage case. If $N\triangle t$ is negligible, the diversity gain comparable to selection combining can be achieved. By configuring different antenna combinations for different retry chains, the antenna combination will be changed within a couple of frame transmissions which is typically few milliseconds or less, so we can make $N\triangle t$ significantly negligible with small N.

AFD of selection combining is derived in [29] for N Rayleigh fading channels, and shown in Fig. 2.5. For balanced case, i.e., average channel gains[8] are equal for all N channels, AFD is inversely proportional to N. For instance, alternative usage of two antenna combinations decreases AFD by 50% compared with one antenna combination. For imbalanced channels, i.e., their exists an imbalance between average channel gains of antenna combinations, the AFD reduction due to the diversity gain decreases as the imbalance increases.

[8] Average channel gain of antenna combination, c, is equal to $\sqrt{\sum_i g_{i,a_i}^2}$.

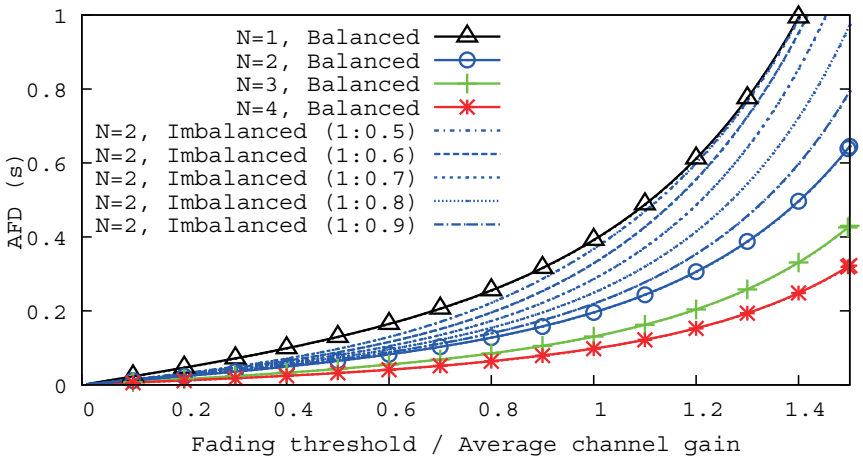

Figure 2.5: Average fade duration of selection combining.

Based on the observations, we propose an algorithm, called Best2Probe, which utilizes the best and 2nd best antenna combinations alternatively. Following the basic procedure of Best1Probe, FSRs of the best (c_{best}), the 2nd best (c_{2nd}), and probed combination (c_{probe}) are measured during T_{interval}, and the best and 2nd best combinations are determined for the next T_{interval}. To compare c_{best} and c_{2nd}, S is configured to either $(c_{\text{best}}, c_{\text{2nd}}, c_{\text{best}}, c_{\text{2nd}})$ or $(c_{\text{2nd}}, c_{\text{best}}, c_{\text{2nd}}, c_{\text{best}})$ alternatively. Moreover, for probing, c_0 is configured to c_{probe} for 10% of the packets. The detailed algorithm is described in Algorithm 2.

Expected problems are the reduction in diversity gain due to the imbalance of channels and the obvious performance degradation when the 2nd best combination is considerably worse than the best one. As described in lines 14–18, therefore, when the gap between the FSRs of the best and 2nd best combinations is larger than a threshold (D_{fsr}),

linesnumbered 2 Best2Probe

```
Set T_interval                                   ▷ set time interval for decision
while transmission do
    timer ← 0
    P_0(c_best), P_0(c_2nd), P_0(c_probe) ← 0 ▷ init. FSR of retry chain 0
    while timer < T_interval do
        if Probing then ▷ 10% of packets are utilized for probing
            S_probe1 ← (c_probe, c_2nd, c_best, c_2nd)   ▷ antenna series for probing
            S_probe2 ← (c_probe, c_best, c_2nd, c_best)
            Use S_probe1 and S_probe2, alternatively
        else
            S_best1 ← (c_best, c_2nd, c_best, c_2nd)     ▷ antenna series for normal
            S_best2 ← (c_2nd, c_best, c_2nd, c_best)
            Use S_best1 and S_best2, alternatively
            if P_0(c_best) − P_0(c_2nd) ≥ D_fsr then
                c_0 ← c_best          ▷ use only the best comb. for retry chain 0
            else if P_0(c_2nd) − P_0(c_best) ≥ D_fsr then
                c_0 ← c_2nd   ▷ use only the 2nd best comb. for retry chain 0
            end if
        end if
        Update P_0(c_best), P_0(c_2nd) and P_0(c_probe)
    end while
    c_best ← arg max_{c_i ∈ {c_best, c_2nd, c_probe}} P_0(c_i)
    c_2nd ← arg max_{c_i ≠ c_best} P_0(c_i)
    Pick new c_probe randomly
end while
```

only the better one is used for retry chain 0 during the remaining time of T_{interval}.

Best2Match: There is a downside of probing at retry chain 0 as Best1Probe and Best2Probe do. A randomly or sequentially se-

lected c_{probe} inevitably degrades the performance because it is less guaranteed to have a good channel condition than the best and 2nd best antenna combinations. Thus, we propose a revised algorithm, called Best2Match, which carries out probing in retry chain 1 and 2 instead of retry chain 0. Since antenna combinations should be compared in the same retry chain, two of the three antenna combinations are compared in each retry chain among retry chains 0–2, and then the performance ranking is determined by the three comparisons as league match. Thus, we configure S to two types as S_{best1}=($c_{\text{best}}, c_{\text{2nd}}, c_{\text{probe}}, c_{\text{best}}$) and S_{best2}=($c_{\text{2nd}}, c_{\text{probe}}, c_{\text{best}}, c_{\text{2nd}}$) as in Algorithm 3. By using the two types of configuration alternatively, c_{best} and c_{2nd} are compared in retry chain 0, c_{2nd} and c_{probe} are compared in retry chain 1, and c_{best} and c_{probe} are compared in retry chain 2. Then, the future c_{best} and c_{2nd} are determined by the results of the three comparisons.

One possible problem with this league match based algorithm is that if c_{best} is in good channel condition, there is no retransmission for S_{best1}, and hence, FSR of c_{2nd} in retry chain 1 cannot be obtained. As a result, c_{2nd} cannot be compared with c_{probe} in retry chain 1 and cannot be updated even though c_{probe} is better than c_{2nd}. In our Best2Match, thus, c_{2nd} is updated to c_{probe} if c_{2nd} is not used due to the relatively low FSR than c_{best} and FSR of c_{probe} in retry chain 1 is equal to 1, i.e., c_{2nd} is in bad channel condition and c_{probe} is expected to be in good channel condition (lines 10–17 and 20–21). The detailed

linesnumbered 3 Best2Match

```
Set T_interval                                   ▷ set time interval for decision
while transmission do
    timer ← 0
    P_i(c_best), P_i(c_2nd), P_i(c_probe) ← 0, i ∈ {0,1,2}
                                                 ▷ init. FSR of retry chain 0, 1, 2
    while timer < T_interval do
        F_update ← false
        S_best1 ← (c_best, c_2nd, c_probe, c_best)
        S_best2 ← (c_2nd, c_probe, c_best, c_2nd)
        Use S_best1 and S_best2, alternatively
        if P_0(c_best) − P_0(c_2nd) ≥ D_fsr then
            c_0 ← c_best   ▷ use only the best comb. for retry chain 0
            if P_1(c_probe) = 1 then
                F_update ← true                  ▷ flag for fast update
            end if
        else if P_0(c_2nd) − P_0(c_best) ≥ D_fsr then
            c_0 ← c_2nd    ▷ use only the 2nd best comb. for retry chain 0
        end if
        Update P_i(c_best), P_i(c_2nd) and P_i(c_probe), i ∈ {0,1,2}
    end while
    if F_update then
        c_2nd ← c_probe
    else
        w_i = arg max_{c_j, i∈{0,1,2}} P_i(c_j)   ▷ find winners of each chain
        c_best ← arg max_{c_j∈{c_best,c_2nd,c_probe}} Σ_i IF(w_i = c_j)
        c_2nd ← arg max_{c_j≠c_best} Σ_i IF(w_i = c_j)
    end if
    Pick new c_probe randomly
end while
```

algorithm is described in Algorithm 3.

The final version of our transmit antenna selection algorithm, Best2Match, has two benefits compared with Best1Probe and Best2Probe. Best1Probe is a baseline algorithm following the basic procedure in [9],

and Best2Probe is an intermediate version.[9] First, Best2Match can reduce the performance degradation due to probing, since it carries out probing only when it is required. Specifically, the probed combination is used for retry chain 1 or 2, which is after all (re)transmissions in retry chain 0 using the best or 2nd best antenna combination have failed, i.e., it is desired to change the corresponding combination. Secondly, it gives more diversity gain by using three combinations for a single packet (N=3 in Fig. 2.5). Packet drop occurs only when all the three antenna combinations are in bad channel condition.

2.4.2 Default Antenna Selection

Different from the transmit antenna selection operated for each station separately, all the associated stations should be considered for default antenna selection. Therefore, it is desirable to select a default antenna combination which performs well universally. Additionally, it is important to give more focus on the stations which show relatively worse performance than others since the stations, which show stable performance with high data rates, tend to be insensitive to antenna combination change. Based on these two factors, we propose a default antenna selection algorithm, called MiDAS (Migratory Default Antenna Selection), as presented in Algorithm 4.

Basically, MiDAS utilizes the result of transmit antenna selection

[9] By comparing Best2Probe and Best2Match, we can separate the gain from the alternative usage of antenna combinations and the gain from the exploitation of multiple retry chains, i.e., league match based algorithms.

linesnumbered 4 MiDAS

```
Set T_window                                          ▷ set time window
K ← T_window/T_interval                               ▷ # of time intervals
for i ← 1...K do
    N_i(c, m) ← 0 ▷ # of selections of antenna combination c with MCS m
end for
while transmission do
    timer ← T_interval
    for j ← timer...1 do
        Update N_K(c, m)        ▷ tracking N_K(c, m) during T_interval
    end for
    c_default ← argmax_c Σ_{i=1}^{K} Σ_{m=0}^{7} N_i(c, m)/R(m)
    for i ← 1...K − 1 do
        N_i(c, m) ← N_{i+1}(c, m)          ▷ memorization for T_window
    end for
end while
```

during the previous time window (T_{window}) to find the most frequently selected antenna combination with all the associated stations. During the i-th T_{interval}, accordingly, MiDAS keeps track of the transmit antenna combination and the MCS used by all the frame transmissions, and then, counts how many times antenna combination 'c' is selected with MCS 'm' ($N_i(c, m)$). At the end of every T_{interval}, an antenna combination, which was used the most for stations with bad channel, during the last T_{window}, i.e., $\text{argmax}_c \sum_{i=1}^{K} \sum_{m=0}^{7} N_i(c, m)/R(m)$ is selected, where K is the number of time intervals in a time window, i.e., $K = T_{\text{window}}/T_{\text{interval}}$. By dividing $N_i(c, m)$ by the corresponding data rate ($R(m)$), we give more weight to the stations in bad channel conditions to enhance their performance.

It is worth mentioning that the default antenna combination selected by MiDAS could operate well not only for multicast and beacon transmission but also for reception since the throughput of DL and UL are highly correlated as discussed in Section 2.3.

2.5 Performance Evaluation

To demonstrate the practicality of the proposed antenna selection algorithms, we have implemented the algorithms in Samsung WEA303 AP. By conducting measurements with the AP and five smartphones (Samsung Galaxy S3), we evaluate the performance of the transmit antenna selection algorithms (Best1Probe, Best2Probe, and Best2Match), and default antenna selection algorithm (MiDAS). The measurements are carried out in the office environment shown in Fig. 2.4, where the stations are placed at four different positions (positions 3–6 in Fig. 2.4). The AP configuration is the same as in Section 2.3.

2.5.1 Performance of Proposed Transmit Antenna Selection

To evaluate the performance of the proposed transmit antenna selection algorithms, we measure the DL UDP throughput for two cases, single station case and multiple station case. In the single station case, only one of the five stations is connected to the AP, where the AP generates DL UDP packets for the station. In the multiple sta-

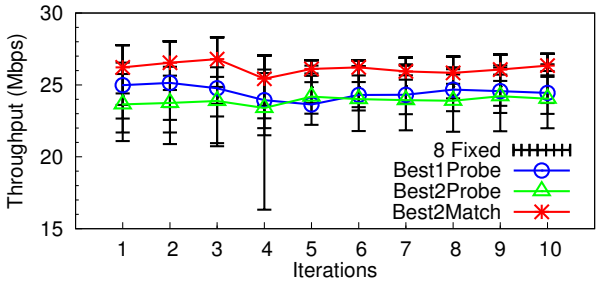

(a) Position 3

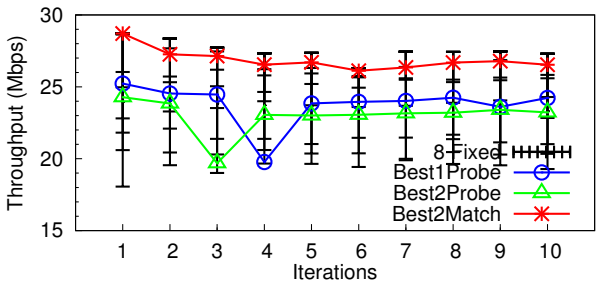

(b) Position 4

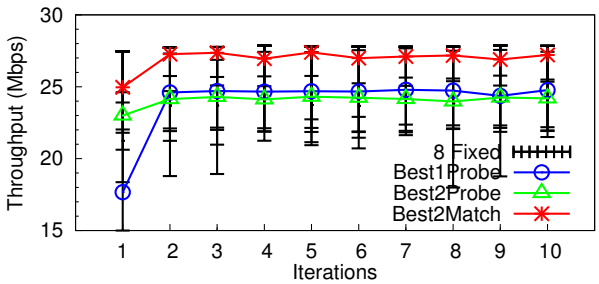

(c) Position 5

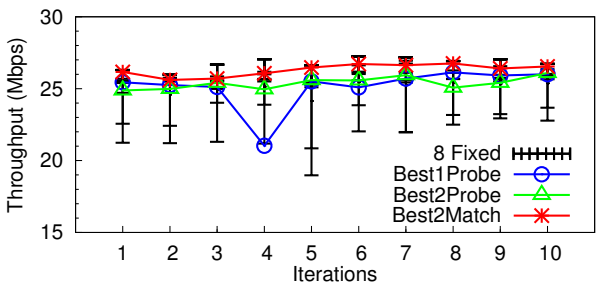

(d) Position 6

Figure 2.6: Temporal throughput change with transmit antenna selection: Single station case.

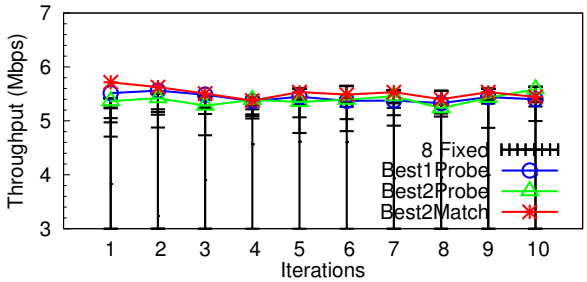

(a) Position 3

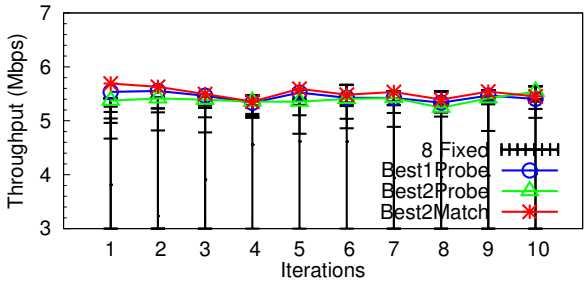

(b) Position 4

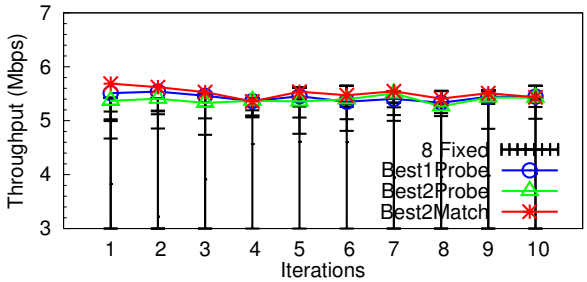

(c) Position 5

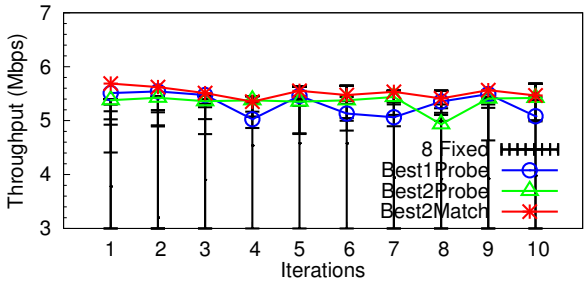

(d) Position 6

Figure 2.7: Temporal throughput change with transmit antenna selection: Multiple station case.

tion case, on the other hand, all the five stations are connected to the AP, and the AP generates DL UDP packets for the five stations with equal source rates. In each case, we measure DL throughput during 30 s repeating for 8 fixed antenna combinations, Best1Probe, Best2Probe, and Best2Match. Therefore, one *iteration* consists of the 11 measurements, and total 10 iterations are carried out for each deployment.[10] As explained in Section 2.3, we make a stationary measurement environment, so channel states are relatively static. The parameters for algorithms are configured as T_{interval}=100 ms, D_{fsr}=0.15, and T_{window}=5 s.

Fig. 2.6 and Fig. 2.7 show the average throughput for each iteration at the four different positions, and it can be interpreted as a temporal throughput change depending on the antenna selection, i.e., fixed, Best1Probe, Best2Probe, or Best2Match. Each bar of 8 Fixed corresponds the throughput of a fixed antenna combination.

In the single station case, there exists a fixed antenna combination which performs the best for each station, and Best2Match is observed to track the best fixed antenna combination properly, while Best1Probe and Best2Probe show performance degradation due to probing even though they track the best antenna combination properly. In the multiple station case, the proposed algorithms are able to achieve higher throughput than the best fixed antenna combination. It is because the best fixed antenna is not the best for each individual

[10]There are five deployments for the single station case while there are only one deployment for the multiple station case.

station while proposed algorithms can track and use the best antenna combination for each station.

In both cases, we observe the gain of Best2Match obtained by eliminating the unnecessary probing. However, due to the static channel condition, we cannot observed the gain from alternative use of two antenna combinations. Thus, we carry out another measurement in a mobile environment. As shown in Fig. 2.4, the station labeled 'M' moves back and forth following the straight red line (about 2 m long). The motion is controlled by a configurable robot car, HBE-RoboCar [30], whose speed can be configured up to 0.5 m/s. To focus on the moving station, no other station is connected to the AP, while the AP transmits DL UDP packets for the station for 30 s.[11] We measure the downlink UDP throughput with 8 different fixed antenna combinations, Best1Probe, Best2Probe, and Best2Match, for 10 iterations.

Fig. 2.8 shows the empirical cumulative distribution functions (ECDF) of the measured throughput in the mobile environment with the speeds of 0.3, 0.4, and 0.5 m/s. For all speeds, there is no performance gain from Best1Probe compared with 8 Fixed. On the other hand, Best2Probe and Best2Match achieve significant enhancement by alternatively using two antenna combinations, whereas the enhancement becomes even larger for higher speed.

The measurement results of the transmit antenna selection algo-

[11] We conduct the measurement with the moving station at edge region to make the environment where the station experiences bad channel frequently.

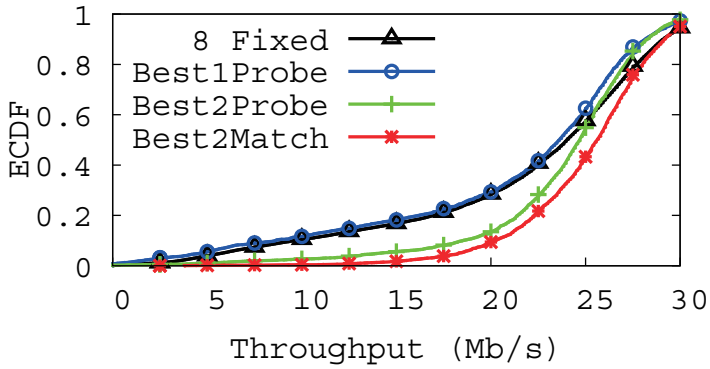

(a) Speed=0.3 m/s

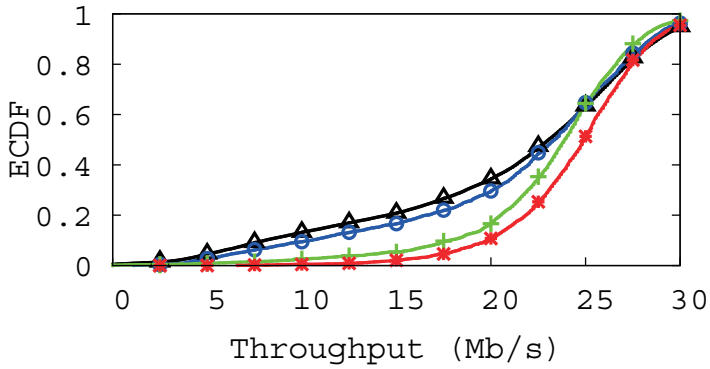

(b) Speed=0.4 m/s

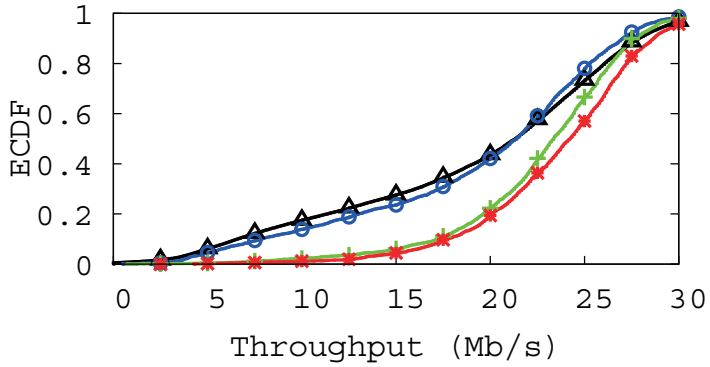

(c) Speed=0.5 m/s

Figure 2.8: Empirical CDF of throughput with three different speeds.

Table 2.4: Summary of transmit antenna throughput.

		8 Fixed	Best1P	Best2P	Best2M	Gain (%)
Static (Mb/s)	Single	24.05	24.51	24.25	26.44	9.95
	Multiple	4.12	5.42	5.36	5.51	33.77
Mobile (Mb/s)	0.3 m/s	21.08	20.81	23.07	24.15	14.55
	0.4 m/s	20.15	20.62	22.39	23.77	17.96
	0.5 m/s	18.70	18.94	21.86	22.94	22.66

rithms in the static and mobile environments are summarized in Table 2.4. The measured throughput of each iteration is averaged, and 8 fixed antenna combinations are averaged together. The gain of Best2Match compared with the average of 8 fixed antenna combinations is also listed in Table 2.4. In the static channel case, Best2Match improves the throughput by about 10.0% and 33.8% compared with the average of 8 fixed antenna combinations for the single station case and for the multiple station case, respectively. In the mobile channel case, Best2Match improves the throughput by about 14.6%, 18.0%, and 22.7% compared with the average of 8 fixed antenna combinations respectively for the speed of 0.3, 0.4, and 0.5 m/s. Due to the limitation of HBE-RoboCar, measurement with the higher speed than 0.5 m/s is not carried out, but the larger enhancement is expected with the typical walking speed over 0.5 m/s. Furthermore, Best2Match is expected to give more performance gain when multiple mobile stations are associated with an AP, which is the typical environment of

infrastructure-based WLAN with smartphones.

2.5.2 Performance of Proposed Default Antenna Selection

To evaluate the default antenna selection algorithm, MiDAS, we compare the downlink multicast throughput of MiDAS with multicast throughputs of 8 different fixed default antenna cases. The AP generates multicast packets for the five stations with source rate of 5 Mb/s, and generates unicast packets for the five stations with 6 Mb/s source rates. The AP uses Best2Match for the transmit antenna selection, which collaborates with MiDAS. We measure the multicast throughput of each station for 30 s, and 10 iterations are carried out in the static channel without mobility.

Fig. 2.9 shows temporal throughput and frame error rate (FER) changes of the worst station, which has the lowest throughput among five stations for each iteration. The default antenna is desired to guarantee the performance of all the associated stations including the stations in bad condition. Therefore, the performance of the worst station is an important factor. For the fixed antenna combination, the throughput and FER vary significantly, and the worst station might not be able to receive the multicast packets with certain default antenna combinations. However, MiDAS closely follows the best antenna combination of the worst station, thus achieving the throughput over 4 Mb/s and FER under 0.2.

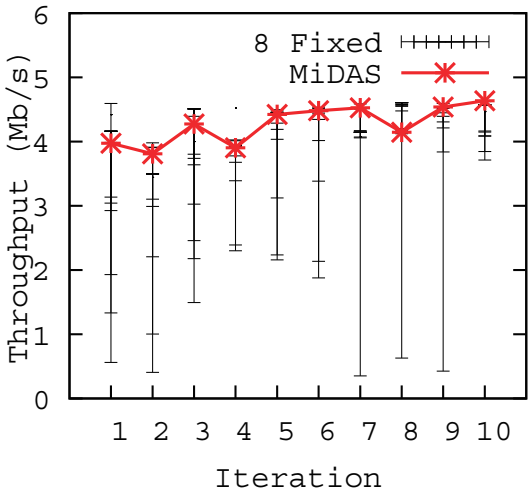

(a) Throughput

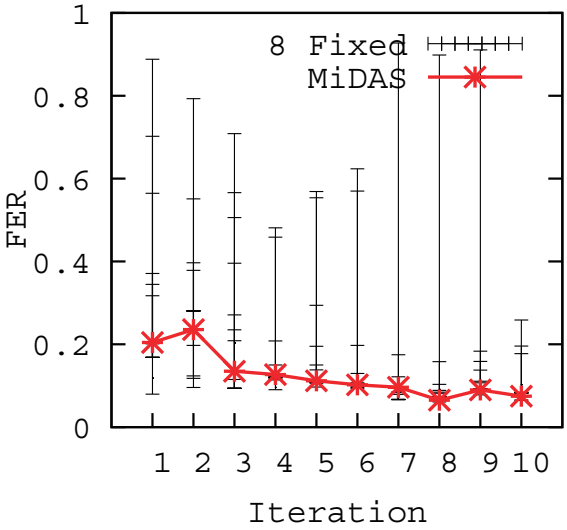

(b) Frame error rate

Figure 2.9: Temporal performance of the worst station with MiDAS in static channel environments.

Table 2.5: Summary of default antenna performance.

	8 Fixed–average	MiDAS	Gain (%)
THR (Mb/s)	3.49	4.30	23.29
FER	0.26	0.12	−53.58

The measurement results of MiDAS including the throughput and FER of the worst station are summarized in Table 2.5. MiDAS improves the throughput of the worst station by about 23.3% and reduces FER by about 53.6% compared with the average of 8 fixed default antenna combinations.

2.6 Summary

We present an antenna selection system for infrastructure-based WLANs, which is applicable to commercial WLAN devices. Practical antenna selection algorithms of AP for unicast/multicast transmission and reception are proposed by considering practical issues. By alternatively using two best antenna combinations and reducing unnecessary probing overhead, the proposed algorithms achieve significant performance gain. The algorithms are evaluated via measurements with prototype implementation in a commercial AP. To the best of our knowledge, we are the first to present antenna selection algorithms without using CSI. We plan to extend our algorithms to incorporate the support of multi-user MIMO in the future.

Chapter 3

Protective Clear Channel Assessment

3.1 Introduction

Spatial reuse is one of the primary interests in wireless local area networks (WLANs) since it greatly improves the network capacity by enabling concurrent transmissions in a shared medium. Especially, promoting spatial reuse is of great importance for densely deployed WLANs, where a number of access points (APs) and their client stations share the medium.

Medium sharing in WLANs is controlled by clear channel assessment (CCA) which determines the availability of wireless medium using carrier sense threshold (CST). Since the CCA highly affects the network capacity, there have been many studies on controlling CST

for efficient medium sharing. Analytic approaches proposed in [10, 11] focus on addressing the hidden terminal problem, which results in a conservative CST to eliminate all possible hidden transmitters in the entire range. Such a conservative CST obstructs concurrent transmissions even when they are possible, i.e., exposed terminal problem. On the other hand, heuristic approaches based on the frame error rate yield a less conservative CST by heuristically considering only some possible hidden transmitters [12, 13].

However, the current CCA method has an inherent limitation in that it utilizes only the received signal strength (RSS) of an incoming frame to determine the availability of the medium. As a result, a carrier sensing node cannot be aware of whether it can transmit along with an ongoing transmission, i.e., a concurrent transmission, which is possible when its transmission will not harm the ongoing transmission from another cell.

In this chapter, we propose a novel CCA mechanism, which overcomes the limitation of the current CCA by exploiting extra information in the physical layer (PHY) header of incoming frames. The performance of the proposed method is evaluated via ns-3 simulator, and the results show that the proposed method yields up to 1.54× throughput compared with the current CCA method by increasing spatial reuse significantly.

The rest of the chapter is organized as follows. In Section 3.2, we introduce the background and motivation of this work. Section 3.3

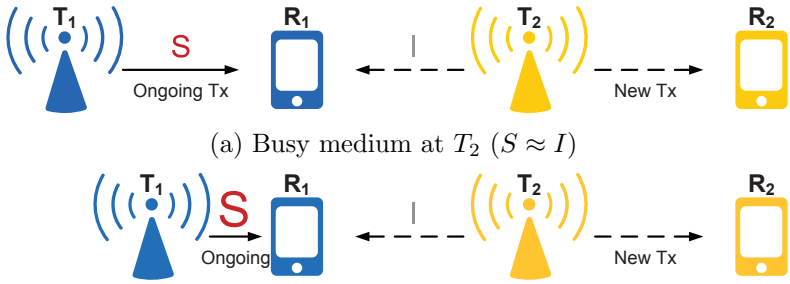

(a) Busy medium at T_2 ($S \approx I$)

(b) Idle medium at T_2 ($S \gg I$)

Figure 3.1: CCA result depending on the possibility of capture effect.

describes the proposed CCA method. Simulation-based performance evaluation is presented in Section 3.4, and Section 3.5 concludes the chapter.

3.2 Background and Motivation

3.2.1 Ideal Operation of CCA

In WLANs, when there is an ongoing transmission, a carrier sensing node senses the medium busy to prevent collision between the ongoing transmission and a new transmission of the carrier sensing node. However, one or both of the colliding frames can be successfully received by virtue of so-called capture effect when the signal strength of a frame is significantly stronger than that of the other. Therefore, CCA should consider the possibility of capture effect to promote spatial reuse.

Fig. 3.1 shows an example of an ideal CCA operation with the

consideration of capture effect. Suppose that there is an ongoing transmission from T_1 to R_1 (frame F_1). As shown in Fig. 3.1(a), the signal quality of the ongoing transmission, i.e., the RSS of F_1, is not high enough to enable R_1 to decode F_1 with the interference from T_2. In this case, a new transmission from T_2 will cause failure of the ongoing transmission. Accordingly, T_2 should determine the medium is busy and defer its transmission. On the other hand, as shown in Fig. 3.1(b), when the signal quality is sufficiently greater than the interference due to the close distance between T_1 and R_1, the ongoing transmission will succeed even if T_2 starts a new transmission. Therefore, T_2 should be able to initiate a new transmission by sensing the medium idle.

The possibility of capture, i.e., the success possibility of ongoing transmission, can be examined by signal-to-interference ratio (SIR) as:

$$\frac{S_{T_1 \to R_1}}{I_{T_2 \to R_1}} \geq \gamma(m_{data,ongoing}), \tag{3.1}$$

where $S_{T \to R}$, $I_{T \to R}$, and $\gamma(m)$ are the signal quality of a frame from T at R, the interference caused by the frame from T at R, and the required SIR to capture the corresponding frame whose date rate is m, respectively. It is worth mentioning that γ depends on both data rate (m) and frame length.

In the example and (3.1), only the capture of ongoing transmission is considered. For a successful concurrent transmission, however,

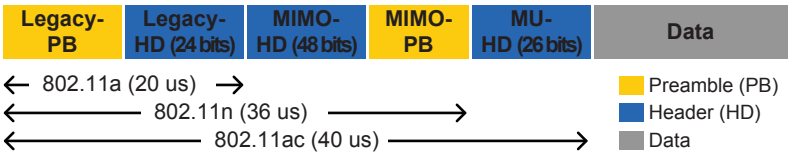

Figure 3.2: IEEE 802.11 physical layer frame format.

the feasibility of a new transmission should be also examined by the following equation:

$$\frac{S_{T_2 \to R_2}}{I_{T1 \to R2}} \geq \gamma(m_{data,new}). \tag{3.2}$$

Furthermore, all data transmissions are followed by ACK frames in WLANs. Accordingly, the feasibility of ACK transmissions should be also examined in a similar way as:

$$\frac{S_{R_1 \to T_1}}{I_{T_2 \to T_1}} \geq \gamma(m_{ack,ongoing}), \tag{3.3}$$

$$\frac{S_{R_2 \to T_2}}{I_{T1 \to T2}} \geq \gamma(m_{ack,new}). \tag{3.4}$$

For an ideal CCA, therefore, T_2 should determine that the medium with an ongoing transmission is idle only when the concurrent transmission is feasible, i.e., all the four equations, (3.1)–(3.4), are satisfied.

3.2.2 IEEE 802.11 Frame Format and CCA Method

Fig. 3.2 shows the PHY frame format of 802.11 frames [23, 24]. In front of data, Legacy-preamble (PB) and Legacy-header (HD) are

attached for 802.11a frames, multiple-input multiple-output (MIMO)-HD and MIMO-PB are further attached for 802.11n frames, and all the shown preambles and headers are utilized for 802.11ac frames.[1]

When a frame is released on the medium, all WLAN nodes who are sensing the medium measure the RSS of the frame at the beginning part of Legacy-PB, and the measured value is compared with CST. If the RSS is greater than CST at a node, the medium is sensed busy by the node.

There is a trade-off for controlling CST. Unnecessarily low CST makes a node sense medium busy and defer its transmission although concurrent transmission is possible, i.e., exposed terminal problem occurs. Unnecessarily high CST, on the other hand, makes a node sense medium idle and start its transmission, although the new transmission causes failure of the ongoing transmission, i.e., hidden terminal problem occurs. Accordingly, high CST reduces the probability of the exposed terminal problem but increases the probability of the hidden terminal problem, and vice versa.

Previous approaches try to control CST to reduce exposed and hidden terminals, but there is an inherent limitation of the CST control. Only the measured RSS of an incoming frame is used for medium sensing, and no other information of the frame is utilized, thus resulting in conservative CCA. For example, if T_2 does not know the signal quality of the ongoing transmission ($S_{T_1 \to R_1}$), T_2 cannot predict whether the

[1]MIMO-HD and MIMO-PB are defined for MIMO operation, and MU-HD is for multi-user MIMO operation.

ongoing transmission will succeed or not (via (3.1)). Consequently, T_2 should determine the medium is busy and defer its transmission to cover the two scenarios illustrated in Fig. 3.1, so spatial reuse cannot be achieved as in Fig. 3.1(b).

Fortunately, we can obtain many types of information from the PHY header. According to 802.11ac standard, which is gaining market share worldwide, all the headers shown in Fig. 3.2 are attached to data. With the three headers, up to 98 bits are available to deliver many types of information such as data rate, frame length, destination ID,[2] etc.

3.2.3 Physical Layer Header Utilization for CCA

Separated from the current CCA using CST, we propose an additory CCA method which is close to the ideal operation of CCA by exploiting the information bits in the PHY header. We assume source ID, destination ID, and signal quality[3] are conveyed in the PHY header to examine the feasibility of concurrent transmission. Detailed algorithm will be described in the following section. It has to be mentioned that the signal quality in the PHY header should be the signal quality of the reverse direction of the frame transmission, i.e., the pre-measured signal quality of a frame from the corresponding destination at the transmitter. It is because the transmitter cannot measure the signal

[2]Partial association ID (PAID) and partial BSSID (PBSSID) are utilized as the destination ID respectively for downlink and uplink.

[3]To embed signal quality, we can exploit the seven reserved bits in PHY header [24] or Spatial Reuse field newly defined in IEEE 802.11 TGax [31].

quality of the frame transmitted by itself, but it can measure only that of the frame it has received. In addition, a frame can be recognized whether it is from own cell, i.e., own basic service set (BSS), or from another cell, i.e., overlapping BSS (OBSS), based on the source and destination IDs since one of them must be the corresponding AP's ID.

3.3 Protective Clear Channel Assessment

In this section, we present the proposed CCA method, namely ProCCA (Protective CCA) to achieve spatial reuse by enabling concurrent transmission only when both ongoing and new transmissions can be protected, i.e., both transmissions are likely to succeed.

ProCCA basically works as follows.

1. *Detection of ongoing transmission:* If there is a frame whose RSS is larger than CST, the reception will be proceeded until the frame's MU-HD is read.

2. *Examination for concurrent transmission feasibility:* If the detected ongoing transmission is from an OBSS node, (3.1)–(3.4) is used to examine the success possibility of the ongoing and new transmissions.

3. *Drop/receive:* If the ongoing and new transmissions are likely to succeed, the incoming frame is dropped, and then the medium is regarded to be idle. Otherwise, the entire frame is received.

Table 3.1: An example of T_2's Signal Quality Table.

BSS	Source	Dest	Signal Quality	RSS
OBSS	T_1	R_1	-45 dBm ($S_{R_1 \to T_1}$)	-65 dBm ($I_{T_1 \to T_2}$)
	R_1	T_1	-40 dBm ($S_{T_1 \to R_1}$)	-70 dBm ($I_{R_1 \to T_2}$)
	T_3	R_3	-50 dBm ($S_{R_3 \to T_3}$)	-80 dBm ($I_{T_3 \to T_2}$)
MYBSS	R_2	me	-40 dBm ($S_{T_2 \to R_2}$)	
	O_2	me	-50 dBm ($S_{T_2 \to O_2}$)	

To check the success possibility of the ongoing and new transmissions, signal quality of the transmissions, and the subsequent ACK transmissions, e.g., $S_{T_1 \to R_1}$, $S_{T_2 \to R_2}$, $S_{R_1 \to T_1}$, and $S_{R_2 \to T_2}$, should be known to the carrier sensing nodes, i.e., T_2. Therefore, we describe how to obtain the signal quality first, and the detail of ProCCA later.

3.3.1 Signal Quality Table

By overhearing transmissions between any two nodes in an OBSS, a carrier sensing node, T_2, can obtain the signal quality between the nodes and measure the RSS of the frames from them. For example, if there is an ongoing transmission from T_1 to R_1, T_2 can measure the RSS of the frame ($I_{T_1 \to T_2}$) and obtain the signal quality of the reverse direction, i.e., the signal quality of the transmission from R_1 to T_1 ($S_{R_1 \to T_1}$), via the PHY header in the frame.

Using the information, the carrier sensing node maintains a table, namely signal quality table, to keep track of signal quality of the OBSS nodes as shown in Table 3.1. The measured RSS of OBSS frames are also tracked to estimate the expected interference to the corresponding

node, e.g., $I_{T_2 \to R_1}$, as explained in the following subsection.

To examine the success possibility of a new transmission, the carrier sensing node also keeps track of the signal quality of its previous transmissions by receiving frames from the corresponding receiver (See Table 3.1). Specifically, it stores $S_{T_2 \to R_2}$ from the PHY header in a frame from R_2.

3.3.2 Feasibility Check of Spatial Reuse

Firstly, the success possibility of ongoing transmission is examined by (3.1) and (3.3). The SIR requirements, $\gamma_{data,ongoing}$ and $\gamma_{ack,ongoing}$, depend on the data rate and length of the ongoing frame, which are delivered in the PHY header. The signal quality, $S_{T_1 \to R_1}$ and $S_{R_1 \to T_1}$, and the RSSs, $I_{R_1 \to T_2}$ and $I_{T_1 \to T_2}$, are listed in the signal quality table as in Table 3.1. Therefore, SIRs of (3.1) and (3.3) can be calculated by using the listed RSSs to estimate interference. For example, if $S_{T_1 \to R_1}$ is -40 dBm and $I_{T_2 \to R_1}$ ($\approx I_{R_1 \to T_2}$) is -70 dBm, SIR of (3.1) is calculated to be 30 dB. For the ease of explanation, we assume a symmetric link for interference, i.e., $I_{A \to B}$ is assumed equal to $I_{B \to A}$. A solution for the practical link asymmetry will be discussed in the following subsection.

If the ongoing transmission is likely to succeed, the success possibility of new transmission is subsequently examined by (3.2) and (3.4). The SIR requirements, $\gamma_{data,new}$ and $\gamma_{ack,new}$ are known to T_2 due to the data rate and length of the new frame are decided by T_2.

linesnumbered 5 Interference Estimation

1: $\hat{I}_{T1\rightarrow R2} \leftarrow {}^{S_{T_2\rightarrow R_2}}/_{\gamma_{data,new}}$ ▷ Initialization to satisfy (3.2)
2: **while** $\Delta RSS_{T1\rightarrow T2} \leq 1$ dB **do** ▷ To check channel variation
3: **if** 3 consecutive concurrent transmission attempts fail **then**
4: $\hat{I}_{T1\rightarrow R2} \leftarrow 3 \times \hat{I}_{T1\rightarrow R2}$ ▷ (3.2) will not be satisfied
5: **end if**
6: **end while**
7: Go to line 1 ▷ Re-initialization to consider the channel variation

The signal quality at R_2 is also listed in Table 3.1, e.g., $S_{T_2\rightarrow R_2}$ is -40 dBm. All the other values in (3.2) and (3.4) are measured by T_2 except the interference at the receiver side, e.g., $I_{T_1\rightarrow R_2}$. The interference at the receiver is not available at T_2, and hence, we estimate it using a heuristic algorithm shown in Algorithm 5.

Algorithm 5 operates as a trial and error approach. The interference, $\hat{I}_{T_1\rightarrow R_2}$, is initially set to a value barely satisfying (3.2) so that T_2 can concurrently transmit with the interference from T_1. If three consecutive concurrent transmission attempts fail, then the estimated interference is increased not to satisfy (3.2), i.e., no more concurrent transmissions. This procedure is restarted when channel varies significantly, i.e., the variation of $RSS_{T1\rightarrow T2}$ exceeds a certain threshold, e.g., 1 dB.

3.3.3 Consideration of Link Asymmetry

Basically, wireless channel is reciprocal, but the RSS is not in general due to the difference of RF parameters between wireless nodes. Accordingly, interference between any two nodes could be different from

each other, e.g., $I_{T_2 \to R_1} \neq I_{R_1 \to T_2}$, which causes inaccurate result from (3.1) and (3.3).

By considering the RF differences, the interference ($I_{T_2 \to R_1}$) can be expressed accurately as follows:

$$I_{T_2 \to R_1} = I_{R_1 \to T_2} \cdot \frac{P_{T_2}}{P_{R_1}} \cdot \frac{G_{R_1}}{G_{T_2}}, \tag{3.5}$$

where P_A is the transmit power of A, and G_A is receive combining gain of A with multiple antennas.[4] G_{R_1} is assumed to be 1, because R_1 already tuned to the frame from T_1, thus yielding marginal gain for the interference from T_2.

SIR at the receiver of the ongoing transmission, therefore, can be expressed as

$$\frac{S_{T_1 \to R_1}}{I_{T_2 \to R_1}} = \frac{(S_{T_1 \to R_1} \cdot P_{R_1})}{(I_{R_1 \to T_2} \cdot P_{T_2})} \cdot G_{T_2}, \tag{3.6}$$

where P_{T_2} and G_{T_2} are known to T_2. Therefore, T_2 can accurately calculate SIR at R_1 if R_1 announces the numerator in (3.6), i.e., $S_{T_1 \to R_1} \cdot P_{R_1}$, instead of announcing signal quality, i.e., $S_{T_1 \to R_1}$, via the PHY header.[5]

[4] Receive combining gain is a diversity gain from MIMO techniques, which varies depending on the number of antennas and receive combining scheme.

[5] We only describe the case of data transmissions of ongoing link since there is no difference with the ACK transmission case.

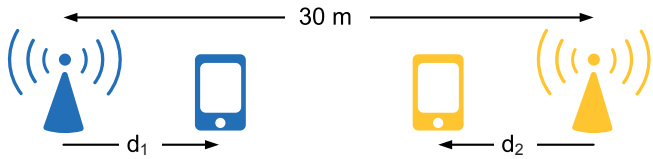

Figure 3.3: Simulation topology for two overlapping cells.

3.4 Performance Evaluation

The performance of the proposed schemes is evaluated via ns-3 simulation [32]. To check whether ProCCA operates as the ideal CCA, we conduct simulation with a simple topology as illustrated in Fig. 4.5. There are two APs 30 m apart from each other (such that the RSS of a frame from an AP at another AP is -64 dBm) and two STAs located d_1 and d_2 away from their associated APs, respectively.

Positive distance refers that the STA is on the side of OBSS, and negative distance means the opposite side of OBSS. For every combination of (d_1, d_2), $d_1, d_2 \in \{-15, -14, \cdots, 13, 14\}$ (m), saturated downlink UDP traffic is generated for both APs and throughput is measured for 1 second. Jakes' fading model is used and other simulation parameters follow those in TGax simulation scenarios [33].

Fig. 3.4, 3.5, and 3.6 shows the throughput for every (d_1, d_2) pair by color at the coordinate; color closer to red represents higher throughput and that closer to blue represents lower throughput. The left diagram shows the aggregate throughput of the two BSSs, and the right diagram shows the minimum throughput among the two BSSs.

In Fig. 3.4, when CST is fixed to -82 dBm, throughput of the

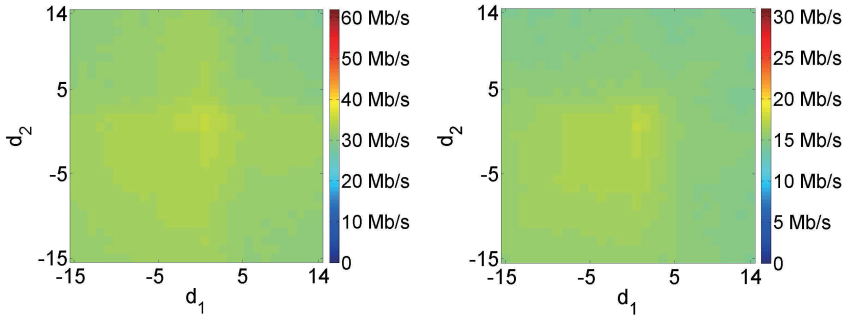

(a) Sum. throughput (b) Min. throughput

Figure 3.4: Performance of Legacy (−82 dBm).

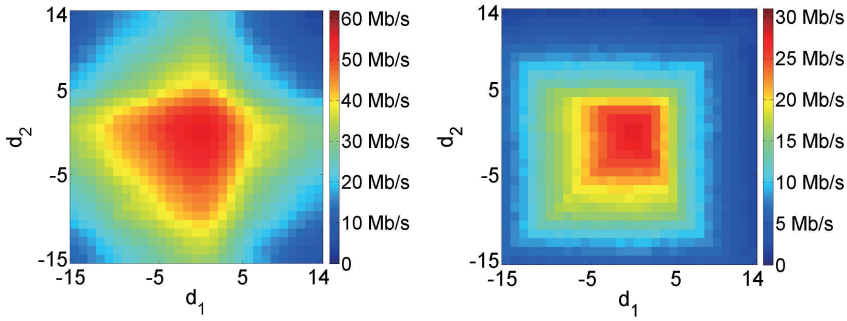

(a) Sum. throughput (b) Min. throughput

Figure 3.5: Performance of Legacy (−62 dBm).

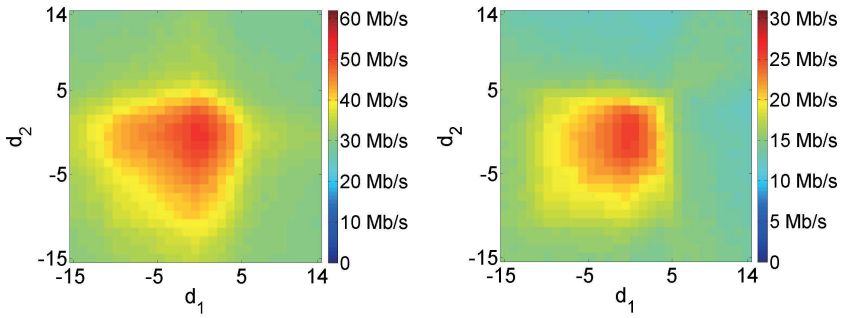

(a) Sum. throughput (b) Min. throughput

Figure 3.6: Performance of ProCCA.

legacy CCA, i.e., the current CCA mechanism, does not depend on the locations of STAs. For every (d_1, d_2), the aggregate throughput is about 32 Mb/s and minimum throughput is about 16 Mb/s. Since the RSS is greater than the CST ($-64 > -82$), the APs fairly share the channel and no spatial reuse is achieved. On the other hand, if CST is fixed to -62 dBm, APs with the legacy CCA do not sense each other ($-64 < -62$), thus transmitting their frames simultaneously. Consequently, the throughput becomes nearly doubled when STAs are close to the associated AP, i.e., concurrent transmission is possible, while throughput drops rapidly due to collision as either STA gets far from the AP as shown in Fig. 3.5.

Meanwhile, as shown in Fig. 3.6, ProCCA works properly as the ideal CCA operation. By ProCCA, concurrent transmission is carried out just as the legacy CCA with -62 dBm CST when it is feasible, otherwise medium is fairly shared as the legacy CCA with -82 dBm CST.

For the evaluation with a general topology, we conduct simulation with two-tier hexagonal cell topology with 19 APs. The adjacent APs are 30 m apart, and a single station is randomly located in each cell. Saturated downlink UDP traffic is generated, and we conduct 100 simulations each with different deployments of stations. Aggregate throughput over 19 cells and bottom 10% throughput are measured. Bottom 10% throughput corresponds to the average throughput of the cells whose throughput is in the bottom 10th percentile among

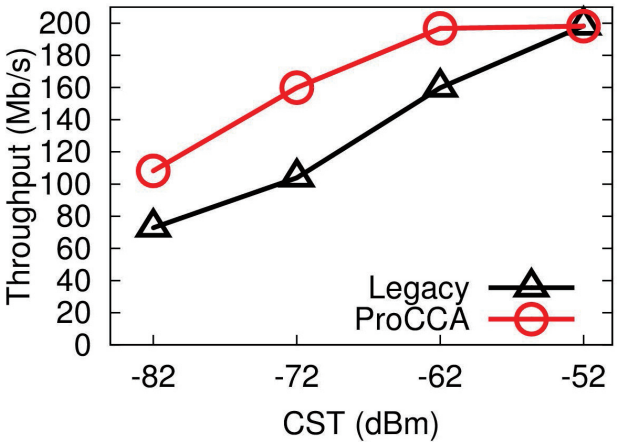

(a) Aggregate throughput

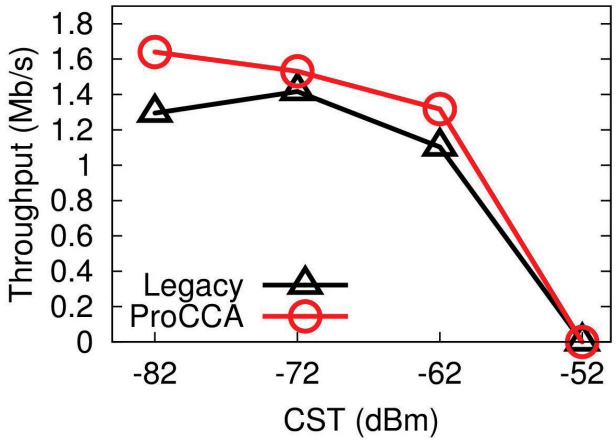

(b) Bottom 10% throughput

Figure 3.7: Performance with two-tier hexagonal cell topology.

the 1900 cells (19 cells and 100 deployments).

As shown in Fig. 3.7, when CST is increased from −82 dBm to −52 dBm, aggregate throughput increases, while bottom 10% throughput decreases. It is because aggressive transmissions with high CST enhance throughput of the cells in good channel state but the cells in bad channel state starves due to many collisions.

ProCCA outperforms the legacy CCA in terms of both aggregated and bottom 10% throughput except when the CST is fixed to −52 dBm, which is a worthless point due to the extreme unfairness, i.e., zero bottom 10% throughput. The aggregate throughput gain over the legacy CCA is 48.6/54.0/24.1% with −82/72/62 dBm CST.

It should be noted that, designed as an additional operation on top of the legacy CCA not to disrupt ongoing transmission, ProCCA is backward comparable with legacy devices, i.e., no concurrent transmission with them, thus not sacrificing them, and does not change the basic operation of the current CCA, i.e., CCA at the beginning of a frame reception.

3.5 Summary

In this chapter, we have proposed a novel CCA mechanism utilizing additional information in the PHY header to examine the feasibility of concurrent transmission. Simulation results demonstrate the proposed scheme significantly enhances network throughput by pro-

moting spatial reuse.

Chapter 4

Dynamic Transmit Power and Data Rate Control

4.1 Introduction

As introduced in the previous chapter, the network capacity of WLANs can be greatly improved by spatial reuse, and a novel CCA mechanism, ProCCA, is proposed for better spatial reuse.

Along with CCA, transmit power and data rate highly affect spatial reuse. By decreasing transmit power of a cell, the interferences from the cell to other cells are reduced, thus results in SINR increase in the other cells. By assuming ideal CCA as introduced in the previous chapter, i.e., medium is determined idle if concurrent transmission is possible with the ongoing transmission, the SINR increase will result in the higher probability of concurrent transmission. However, the

transmit power decrease can induce frame error of the corresponding cell. Therefore, there is a trade-off between reliability and spatial reuse with transmit power control.

Meanwhile, the probability of concurrent transmission can be also increased by lowering data rate because SINR requirement for a successful transmission decreases as data rate decreases, but the lowered data rate directly affects on the transmission time. Transmission time increases as data rate decreases, which can result in throughput degradation. Thus, there is another trade-off between spatial reuse and transmission time with data rate control.

Accordingly, there have been many researches on transmit power control to promote spatial reuse, but existing power controls operate in a conservative manner. Concurrent transmission is meaningful only when the simultaneously transmitted frames are successfully received via capture effect, and it depends on the transmitters and receivers of the concurrent transmission. Previously, WLAN nodes cannot know the transmitter and receiver of ongoing transmission before receiving and decoding the packet, i.e., the nodes do not know exactly which node will transmit simultaneously with them. Therefore, a WLAN node should consider all the possible transmitters in a topology or in an analytical region to select its transmit power which result in a conservative operation.

To solve this problem, we propose a dynamic transmit power and rate control algorithm which exploits PHY header to recognize the

transmitter and receiver of ongoing transmission and obtain the signal quality among them as introduced in the previous chapter. Our proposed algorithm dynamically adapts the transmit power and data rate depending on the ongoing transmission if any ongoing transmission is detected before its transmission. The performance of the proposed algorithm is evaluated via ns-3 simulator, and the results show that the proposed algorithm enhances network performance compared with ProCCA by promoting more concurrent transmissions.

The rest of this paper is organized as follows. In Section 4.2, we introduce the existing transmit power and data rate control algorithms for spatial reuse. Section 4.3 describes our proposed transmit power and data rate control algorithm, and simulation-based performance evaluation is presented in Section 4.4. Finally, Section 4.5 summarizes the chapter.

4.2 Transmit Power and Rate Control for Spatial Reuse

By enabling concurrent transmission when the colliding frames can be captured, the achievable throughput of WLANs is significantly enhanced as described in Chapter 3. Therefore, we propose a new CCA mechanism (ProCCA) which determines the feasibility of concurrent transmission, i.e., the possibility of the successful capturing, and the status of the medium based on the feasibility.

Meanwhile, the feasibility of concurrent transmission changes according to the transmit powers and data rates of the contending nodes. Accordingly, there have been many researches on transmit power control for spatial reuse, and they can be classified in two categories, namely RTS-CST based and feedback based as described in the following subsections.

4.2.1 RTS-CTS Based

Several papers try to reduce transmit power of data transmissions while avoiding the collision from hidden nodes by differentiating the power of RTS-CTS and data-ACK transmissions. In [14], RTS-CTS packets are transmitted with the maximum power, and the transmit powers of data-ACK packets are reduced accordingly to avoid hidden collisions. The authors in [15] extend the work in [14], and they also control the transmit power of RTS/CST packets considering the transmission range and interfering range to avoid hidden collisions but enhance spatial reuse.[1] However, these approaches are conservative to enabling concurrent transmissions due to RTS-CTS packets are exchanged with high power considering all the possible interfering nodes in the interfering range, which are not always exist.

[1]Interference range of a node is a mathematically defined range where the nodes in the rage can cause the failure of the node's transmission.

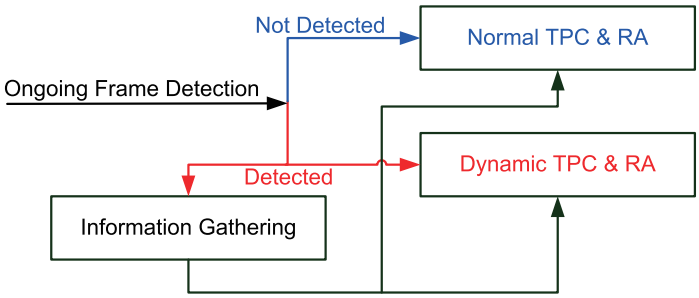

Figure 4.1: Overall structure of DynamicReuse.

4.2.2 Feedback Based

To exploit spatial reuse by enabling concurrent transmissions without the loss from hidden terminals, the feedback based approach tries to find received signal strengths (or allowable interference levels) among the nodes operating in the same medium [16, 17, 18]. The received signal strength (or allowable interference level) of a receiver node is fed back to the corresponding transmitter node, e.g., via an out-of-band channel in [16], a separate control channel in [17], or RTS/CTS exchange at access window in [18], and a transmitter decides it's proper transmit power. When the transmitter decides the transmit power, it considers all the possible future interferers in the medium because all the interferers can corrupt the transmission, and the transmitter does not know who will corrupt the transmission in presence.

4.2.3 Limitations of existing approach

As described in the previous subsections, existing approaches of transmit power control operate in conservative manners, RTS/CST based approach considers all possible interferers in the interfering range and feedback based approach considers all possible interferers in the same medium. It is mainly due to the transmitters do not know when an interferer transmits and corrupts the transmission.

Existing data rate control focus on finding an appropriate data rate based on the channel condition (without interference), and there are a limited number of researches on data rate control for spatial reuse [19, 20]. In [20], the authors lower the data rate to fully exploit the medium even if there are throughput degradation with the lowered rate. The authors in [19] also lower the data rate to tolerate interference even though throughput is possible to decrease. The main limitation of existing data rate control is the throughput degradation with the lowered data rate to exploit spatial reuse.

To solve the limitation of existing transmit power control algorithms, i.e., the conservative operation, we propose our algorithm exploits PHY header information as in Chapter 3, so that a node adapts the transmit power depending on the transmitter and receiver of the ongoing transmission, which are the exact interferers when the node transmit it's packet simultaneously.

For the better spatial reuse, furthermore, the node should lower it's data rate so that the corresponding receiver is supposed to cap-

ture and successfully receive the packet from the node considering the interference from the ongoing transmission. However, the lowered rate is possible to decrease throughput with the increased transmission time. In our proposed algorithm, the node adapts the length of the packet, if the data rate is lowered, in order to eliminate the throughput loss with the lowered data rate. Detailed operation of our proposed algorithm will be described in the next section.

4.3 Dynamic Transmit Power and Rate Control

In this section, we describe the proposed transmit power and rate control algorithm, namely DynamicReuse, which dynamically adapts transmit power and data rate depending on the ongoing transmission by utilizing the information delivered in PHY header. As shown in Fig.4.1, DyanamicReuse consists of three main parts, Information Gathering, Normal TPC & RA, and Dynamic TPC & RA.

Basically, if a node detects ongoing transmission before it's transmission, the transmit power and data rate are controlled depending on the ongoing transmission via Dynamic TPC & RA. If there is no detected ongoing transmission, on the other hand, the node uses the transmit power and data rate which are determined by normal TPC & RA. Both of Dynamic and Normal cases utilize the gathered information which is delivered in PHY header of previously detected

Table 4.1: An example of T_2's Signal Quality Table.

BSS	Source	Dest	Signal Quality (dBm)	RSS (dBm)
OBSS	T_1	R_1	-45 ($S_{R_1 \to T_1} \cdot P_{T_1}$)	-65 ($I_{T_1 \to T_2}$)
	R_1	T_1	-40 ($S_{T_1 \to R_1} \cdot P_{R_1}$)	-70 ($I_{R_1 \to T_2}$)
	T_1	O_1	-45 ($S_{O_1 \to T_1} \cdot P_{T_1}$)	-65 ($I_{T_1 \to T_2}$)
	O_1	T_1	-40 ($S_{T_1 \to O_1} \cdot P_{O_1}$)	-70 ($I_{O_1 \to T_2}$)
	T_3	R_3	-50 ($S_{R_3 \to T_3} \cdot P_{T_3}$)	-80 ($I_{T_3 \to T_2}$)
MYBSS	R_2	me	-40 ($S_{T_2 \to R_2} \cdot P_{R_2}$)	
	O_2	me	-50 ($S_{T_2 \to O_2} \cdot P_{O_2}$)	

transmissions.

4.3.1 Information Gathering

As described in Chapter 3, a node can obtain the information such as source ID, destination ID, and signal quality between the source and destination, via PHY header of previously detected transmissions so that the node can examine the feasibility of concurrent transmission. For DynamicReuse, each node also gathers the information and maintains it's signal quality table via Information Gathering part.

Table. 4.1 shows another example of T_2's signal quality table. Specifically, there are two OBSSs, one consists of T_1, R_1, and O_1, and the other consists of T_3 and R_3, while T_2 has two different destinations, i.e., R_2 and O_2.

Assume that T_2 detects the ongoing transmission from T_1 to R_1. To fully exploit spatial reuse, the transmit power and data rate of T_2 are adapted depending on the source (T_1) and destination (R_1) nodes of the ongoing transmission and it's destination (R_2) considering the

feasibility condition of concurrent transmission as followings:

$$\frac{S_{T_1 \to R_1}}{I_{T_2 \to R_1}} = \frac{S_{T_1 \to R_1} \cdot P_{R_1}}{I_{R_1 \to T_2} \cdot P_{T_2}} \geq \gamma(m_{data,ongoing}), \tag{4.1}$$

$$\frac{S_{R_1 \to T_1}}{I_{T_2 \to T_1}} = \frac{S_{R_1 \to T_1} \cdot P_{T_1}}{I_{T_1 \to T_2} \cdot P_{T_2}} \geq \gamma(m_{ack,ongoing}), \tag{4.2}$$

$$\frac{S_{T_2 \to R_2}}{I_{T1 \to R2}} = \frac{S_{T_2 \to R_2} \cdot P_{R_2}}{I_{T_1 \to R_2} \cdot P_{R_2}} \geq \gamma(m_{data,new}), \tag{4.3}$$

$$\frac{S_{R_2 \to T_2}}{I_{T_1 \to T_2}} \geq \gamma(m_{ack,new}). \tag{4.4}$$

To accurately estimate the strengths of interference to the ongoing transmission, i.e., $I_{T_2 \to T_1}$ and $I_{T_2 \to R_1}$, by using the measured RSSs of the packets from the transmitter and receiver of the ongoing transmission, i.e., $I_{T_1 \to T_2}$ and $I_{R_1 \to T_2}$, even if the links are asymmetric, PHY header delivers the product of signal quality and the transmit power of the transmitter, i.e., $S_{T_1 \to R_1} \cdot P_{R_1}$ and $S_{R_1 \to T_1} \cdot P_{T_1}$, as described in the previous chapter. Then, all the values including the products of each signal quality and power ($S \cdot P$), interferences (I), and data rates (m), are gathered via PHY header or measured by T_2 itself and listed in T_2's signal quality table except the interference experienced by T_2's destination, i.e., $I_{T_1 \to R_2}$.

To know the accurate strength of interference at the destination, i.e., $I_{T_1 \to R_2}$, we propose a feedback mechanism as illustrated in Fig. 4.2. Basically, the receiver which successfully receives the packet destined to it after second capture[2], feeds back the measured interference from

[2]When a captured packet is received first at the corresponding receiver, it is

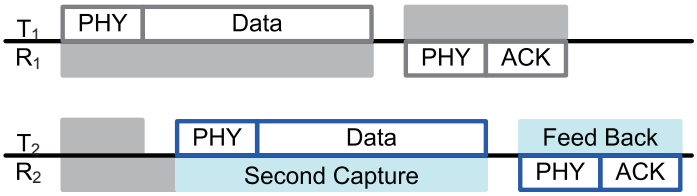

Figure 4.2: RSS of previous packet feedback after second capture.

the corresponding ongoing transmission which is overheard before the capturing.

As shown in the figure, T_1 firstly occupies the medium, so all the other nodes, i.e., R_1, T_2, and R_2, start to receive the packet from T_1. After decoding PHY header, T_2 determines that the concurrent transmission is feasible, so it transmits it's packet after back-off. Then, R_2 starts to receive the packet from T_2 by second capture. Before the capturing, R_2 already measured the RSS of the packet from T_1, so that R_2 can feedback $I_{T_1 \rightarrow R_2}$ to T_2 via ACK packet.

In the following two subsections, the way how to control the transmit power and data rate using the inequalities to examine the feasibility of concurrent transmission will be described. For the ease of explanation, we focus on T_2's transmit power and rate control, i.e., control of P_{T_2} and $m_{data,new}$, which can be applied to any nodes.

first capture, while the captured packet is received after the colliding packet, it is second capture [34].

4.3.2 Dynamic TPC & RA

By reducing transmit power, i.e., P_{T_2}, the strength of interference to the ongoing transmission, i.e., $I_{T_2 \to T_1}$ and $I_{T_2 \to R_1}$, decreases so that the ongoing transmission can succeed while the reliability of T_2's transmission is also decrease. Therefore, T_2 calculates the transmit power, $P_{reduced}$, barely satisfying the equations (4.1) and (4.2) as follows:

$$P_{reduced,data} = \frac{S_{T_1 \to R_1} \cdot P_{R_1}}{I_{R_1 \to T_2} \cdot \gamma(m_{data,ongoing})} - M, \tag{4.5}$$

$$P_{reduced,ack} = \frac{S_{R_1 \to T_1} \cdot P_{T_1}}{I_{T_1 \to T_2} \cdot \gamma(m_{ack,ongoing})} - M, \tag{4.6}$$

$$P_{reduced} = min(P_{reduced,data}, P_{reduced,ack}), \tag{4.7}$$

where M denotes a configurable margin to surely hold the inequalities.

Meanwhile, the signal quality, i.e., $S_{T_2 \to R_2}$, also decreases along with $P_{reduced}$, thus might result in the failure of T_2's transmission. By lowering the data rate, T_2 can enhance the reliability, i.e., the capture threshold (γ) is reduced along with the lowered rate. Therefore, T_2 finds the data rate, $m_{reduced}$, which is supposed to hold the inequality (4.3) with the reduced power as follows:

$$\frac{S_{T_2 \to R_2}}{I_{T_1 \to R_2}} \cdot \frac{P_{reduced}}{P_{T_2}} \geq \gamma(m_{reduced}). \tag{4.8}$$

However, the lowered data rate increases the transmission time of T_2's packet, so it is possible to even degrade the throughput of T_2 by concurrent transmissions with the lowered rate.

To get a better understanding, we analyze the distributed coordination function (DCF) throughput which will be presented in 4.3.4. Based on the throughput analysis, the packet size of T_2 should be adapted when the data rate is lowered so that the concurrently transmitted packets end at the same time.

4.3.3 Normal TPC & RA

In the previous subsection, the transmit power and rate control for concurrent transmission with the detected ongoing transmission is described. By reducing the transmit power for normal transmission, i.e., when no ongoing transmission is detected, spatial reuse can be more exploited. For example, if T_1 transmits the packet with reduced power, the interference to T_2 and R_2 is decreased, which results in the higher probability for concurrent transmission with T_2. Therefore, we introduce how to control the transmit power for normal transmission while the data rate for normal transmission is controlled appropriately with existing approaches, e.g., ARF, Mistrel, etc, considering channel variations.

To support the maximum data rate even though there is a back-off collision,[3] in DynamicReuse, each node finds the transmit power

[3]Back-off collision denotes the concurrent transmission of the transmitters who

which is supposed to support the maximum data rate (m_{max}) considering all the possible interference from observed OBSS nodes. Accordingly, for each OBSS transmitter (T_{obss}), the minimum transmit power ($P_{required}(T_{obss})$), which is required to support the maximum data rate, is calculated as follows:

$$P_{required}(T_{obss}) = \gamma(m_{max}) \cdot P_{previous} \cdot \frac{I_{T_{obss} \rightarrow R_2}}{S_{T_2 \rightarrow R_2}}, \tag{4.9}$$

where $P_{previous}$ is the lastly used transmit power for the packet to R_2, which is corresponds to the $S_{T_2 \rightarrow R_2}$. Then, the minimum required power considering all the interferers ($P_{required}$) is calculated as:

$$P_{required} = max_{T_{obss} \in \{S_{obss}\}} P_{required}(T_{obss}) \tag{4.10}$$

where S_{obss} denotes the set of OBSS transmitters, e.g., $S_{obss} = \{T_1, R_1, O_1, T_3\}$ for T_2 as listed in Table. 4.1.

4.3.4 DCF Throughput Analysis

In this subsection, we analyze per-node DCF throughput of two cases, medium shared case and spatial reuse case, to verify the trade-off between spatial reuse and transmission time depending on data rate, e.g., concurrent transmission becomes possible with lowered data rate, but transmission time increases with the lowered data rate.

Medium shared case: When two nodes, namely node A and B,

pick the same back-off counter values

Table 4.2: An example of back-off counter change.

Round	1	2	3	4	5	...
X	**10**	7	2	**10**	**3**	...
Y	**3**	**5**	**12**	10	**9**	...

are contending to transmit their packets, the probability to win the contention is varies depending on their back-off counter values. Let us denote X and Y are back-off counter values at the beginning of an idle slot after any node's transmission denoted by *round*. Then, X and Y depend on the previous round. The winner, which has the smaller back-off counter value, of the previous round renews its back-off counter by random pick in the range of $[0,W-1]$, while the loser's back-off counter value is equal to the difference between their previous back-off counter values. When the back-off counter values of them are the same, both of the back-off counter values are renewed together. Table 4.2 illustrates an example of back-off counter sequences for each round.

Expected time for a round, $E[\text{Time for a round}]$ can be obtained

as follows:

$$
\begin{aligned}
E[\text{Time for a round}] = \\
P(X<Y)T_A + P(X<Y)E[X|X<Y]\sigma \\
+P(X>Y)T_B + P(X>Y)E[Y|X>Y]\sigma \\
+P(X=Y)max(T_A,T_B) + P(X=Y)E[Y|X=Y]\sigma \\
= P(X<Y)(T_A+T_B) + P(X=Y)max(T_A,T_B) \\
+E[min(X,Y)]\sigma,
\end{aligned}
\tag{4.11}
$$

where σ is a slot time, and T_i is the transmission time for a packet of node i, which is equal to $T_i = T_{DIFS} + T_{DATA} + T_{SIFS} + T_{ACK}$. T_{DIFS} and T_{SIFS} are the DIFS and SIFS deferrals, and T_{DATA} and T_{ACK} denote the transmission time for the data packet and the corresponding ACK packet including PHY and MAC headers [35]. T_{DATA} varies according to the payload size in bits (L) and the data rate (m) of the data packet, which can be calculated as:

$$T_{DATA} = T_{PHY} + \left\lceil \frac{L + L_{add}}{m \cdot T_{symbol}} \right\rceil \cdot T_{symbol}, \tag{4.12}$$

where T_{symbol} denotes the OFDM symbol interval, and T_{PHY} is the duration for PHY including PLCP preamble and PLCP header (except SERVICE field) [23]. L_{add} is the additional bits including MAC header, the SERVICE field, FCS, and Tail bits [35]. The description and value of each parameter are listed in Table. 4.3.

There is an important fact that the average back-off counter value

Table 4.3: Summary of IEEE 802.11 parameters.

Parameter	Value	Description
σ	9 us	slot time
T_{SIFS}	16 us	SIFS time
T_{DIFS}	34 us	DIFS time
T_{PHY}	40 us	duration of PHY (preamble and header)
L_{add}	342 bits	additional bits (MAC and PHY headers)

per transmission of each node is equal to the average of randomly chosen back-off counter values, i.e., $E[B] = \frac{W-1}{2}$. By utilizing it, we can simply calculate the average length of idle time, i.e., average duration for back-off before a transmission, as follows:

$$E[min(X,Y)] = E[B]P(X \leq Y) = \frac{W-1}{2}P(X \leq Y) \tag{4.13}$$

There is another important fact that the probability that back-off counters are the same is $\frac{1}{W}$. Therefore, we can easily obtain $P(X \leq Y)$ as:

$$\begin{aligned} P(X \leq Y) &= P(X = Y) + P(X < Y) \\ &= \frac{1}{W} + \frac{1}{2}(1 - \frac{1}{W}) = \frac{W+1}{2W} \end{aligned} \tag{4.14}$$

Next, we easily obtain the per-node throughput, i.e., S_A and S_B, as follows:

$$S_A = \frac{P(X \leq Y)L}{E[\text{Time for a round}]}, \tag{4.15}$$

$$S_B = \frac{P(X \geq Y)L}{E[\text{Time for a round}]}. \tag{4.16}$$

If the transmission times of node A and node B are the same due to the same data rate, i.e., $T_A = T_B$, per-node throughput is simplified as follows,

$$S_A = \frac{P(X \leq Y)L}{T_A + E[min(X,Y)]\sigma} = S_B. \tag{4.17}$$

When the medium is shared by the two nodes without spatial reuse, one of the nodes transmits its packet with the probability $P(X \leq Y)$ as shown in (4.17).

Spatial reuse case: In spatial reuse case, the loser node, which has the larger back-off counter value, also transmits it's packet along with the winner after deferring it's residual back-off counter value, which is same as the DCF throughput when there is only a single node in the medium as follows:

$$\begin{aligned} S_A &= \frac{P(X \leq Y)L + P(X > Y)L}{E[min(X,Y)] + E[B_{residual}]\sigma + T_A} \\ &= \frac{L}{E[B]\sigma + T_A}, \\ S_B &= \frac{L}{E[B]\sigma + T_B}, \end{aligned} \tag{4.18}$$

where $B_{residual}$ is the residual back-off counter value of the loser ($E[B_{residual}] = E[B] - E[min(X,Y)]$).

Spatial reuse with a lowered rate: Now, we are ready to com-

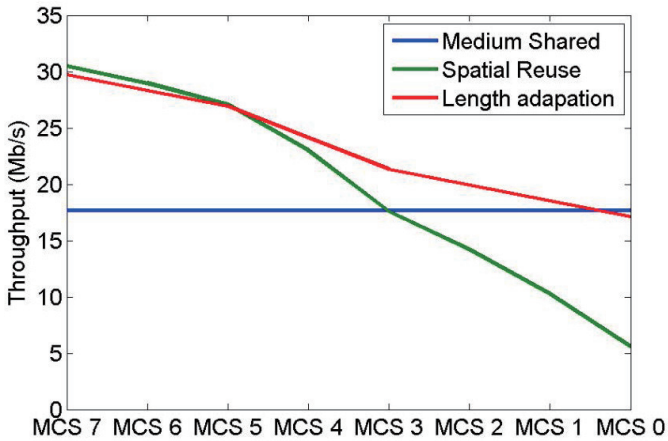

Figure 4.3: DCF throughput with lowered data rate.

pare the DCF throughput with/without spatial reuse via rate lowering. Assume the two nodes, A and B, can utilize the maximum data rate m_{max} if there is no interference, but the transmissions will fail if they transmit simultaneously. Further assume that concurrent transmission is possible if node A lowers it's data rate to $m_{reduced}$ (and it's transmit power) as described in 4.3.2.

Fig. 4.3 shows the DCF throughput of node A, when m_{max} is MCS 7 and $m_{reduced}$ ranges from MCS 7 to MCS 0. Blue line shows the throughput of medium shared case without rate lowering while Green line shows the throughput of spatial reuse case with the lowered rate. There is a crossing point of two lines due to the trade-off between spatial reuse and transmission time depending on data rate. Specifically, it is from the difference between (4.17) and (4.18). Node A can transmit more bits of $P(X > Y)L$ by spatial reuse but the

transmission time, T_A increases with the lowered rate.

Spatial reuse with length adaptation: If we adapt packet length of the loser node, we can obtain the spatial reuse gain without the throughput loss due to the increased transmission time. Specifically, the node who is the winner of the round, i.e, the node who has the smaller back-off counter value, transmits it's packet, while the other node transmit it's packet with reduced packet length where the length is adapted so that the transmission ends before the end of the winner node's transmission. Then, the throughput of node A can be obtained as follows:

$$S_A = \frac{P(X \leq Y)L + P(X > Y)E[G]}{E[min(X,Y)] + E[B_{residual}]\sigma + T_A}, \tag{4.19}$$

where $E[G]$ represents the average payload size (in bits) of the packet whose length is adapted which can be obtained using an inequality as follows:

$$\begin{aligned} T_A(m_{max}) - \frac{E[B_{residual}]}{P(X > Y)} &\geq T_A(m_{reduced}) \\ &= T_{PHY} + \left\lceil \frac{E[G] + L_{add}}{m_{reduced} \cdot T_{symbol}} \right\rceil \cdot T_{symbol}, \end{aligned} \tag{4.20}$$

where $T_A(m)$ represents the transmission time of node A with the corresponding data rate, m.

It should be noted that T_A in (4.19) is the transmission time with m_{max}, i.e., $T_A(m_{max})$, while T_A in (4.18) is the increased transmission time with $m_{reduced}$, i.e., $T_A(m_{reduced})$, which shows there is no

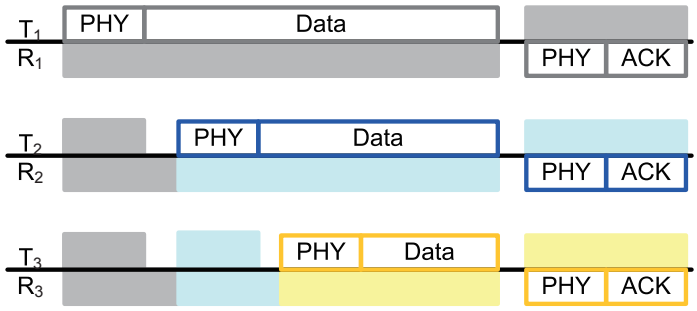

Figure 4.4: Multicell example of DynamicReuse.

increase of transmission time for spatial reuse with the packet length adaptation.

The red line in Fig. 4.3 show the throughput of spatial reuse when the packet length is adapted, and it is verified that the throughput is always enhanced by spatial reuse compared with medium shared case.

4.3.5 Multi-cell Consideration

DynamicRuese operates based on the SIR values and corresponding capture thresholds between the ongoing transmission and the new transmission of a CCA node, e.g., T_2. If more than two nodes transmit their packets concurrently via DynamicReuse, the transmissions could fail due to the superposed interference from the other OBSSs.

Fig. 4.4 illustrates an example of DynamicReuse with three OBSSs. T_1 firstly transmits it's packet to R_1, and T_2 and T_3 decode the PHY header of the packet and determine they can transmit concurrently with the transmission of T_1. After back-off, T_2 transmits it's packet to R_2, and T_3 decodes the PHY header of T_2's packet and de-

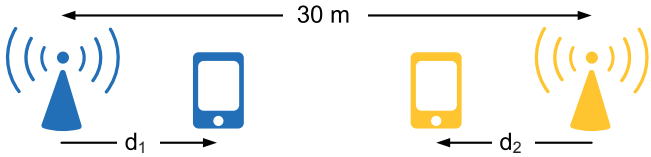

Figure 4.5: Simulation topology for two overlapping cells.

termines that the concurrent transmission with T_2 is feasible. Lastly, T_3 transmits it's packet to R_3. When T_2 and T_3 examine the feasibility of concurrent transmission, the interference should consider the other possible concurrent transmissions due to the interference is superposed, e.g., T_1 interfered by T_2 and T_3 together.

To consider the superposed interference, DynamicReuse controls the capture threshold depending on the observed number of contending OBSSs. For example, the observed number of contending OBSSs of T_2 are two, one with T_1, R_1, and O_1, and the other with T_3 and R_3 as shown in Table. 4.1. It is supposed to be only a single transmission in an OBSS, T_2 would interfere with two OBSS at maximum. Accordingly, the capture thresholds are doubled for T_2. If the number of observed OBSSs is four, the capture thresholds will be threefold, and so on.

4.4 Performance Evaluation

The performance of the proposed scheme is evaluated via ns-3 simulation [32]. To compare DynamicReuse with ProCCA and legacy CCA, we conduct simulation with the two cell topology as illustrated

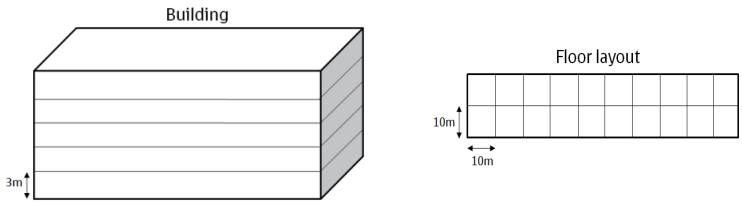

Figure 4.6: Residential building topology for high density environment.

Table 4.4: Simulation parameters for residential building topology.

Data rates	MCS 0–7
Guard interval	Short (0.4 μs)
Tx power	20 dBm
Frame aggregation	No / A-MPDU[4]
Rate control algorithm	Minstrel

in Fig. 4.5, where the simulation parameters are the same as described in the previous chapter, and the result is illustrated in Fig. 4.9.

As shown in Fig. 4.7, Fig. 4.8, and Fig. 4.9, ProCCA enhances the throughput (compared with legacy CCA) by accurately determining the feasible region of concurrent transmission with the detected ongoing transmission, while DynamicReuse increases the feasible region of concurrent transmission (compared with ProCCA) by dynamically adapting the transmit power and data rate depending on the ongoing transmission. Accordingly, DynamicReuse outperforms ProCCA and legacy CCA in terms of both aggregated and minimum throughput.

To evaluate DynamicReuse in high density WLAN environment,

[4]The maximum available length and maximum available time for A-MPDU are 1,048,575 bytes and 5.484 μs, respectively.

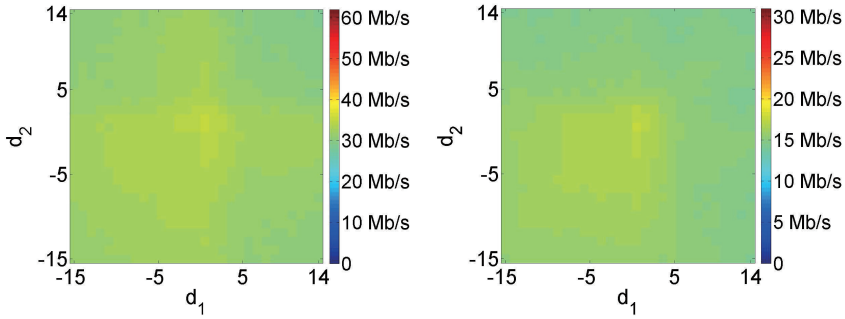

(a) Sum. throughput (b) Min. throughput

Figure 4.7: Performance of Legacy (−82 dBm).

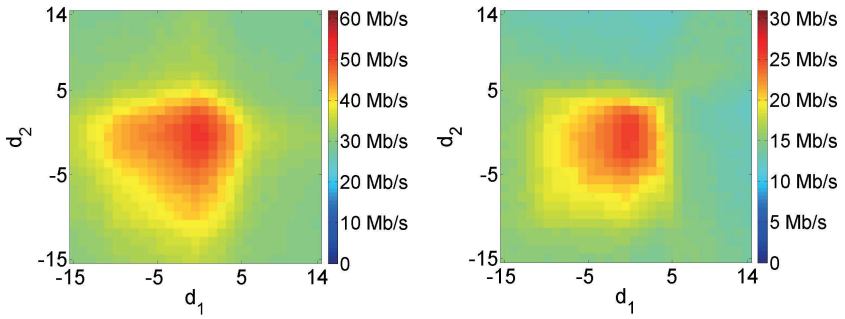

(a) Sum. throughput (b) Min. throughput

Figure 4.8: Performance of ProCCA.

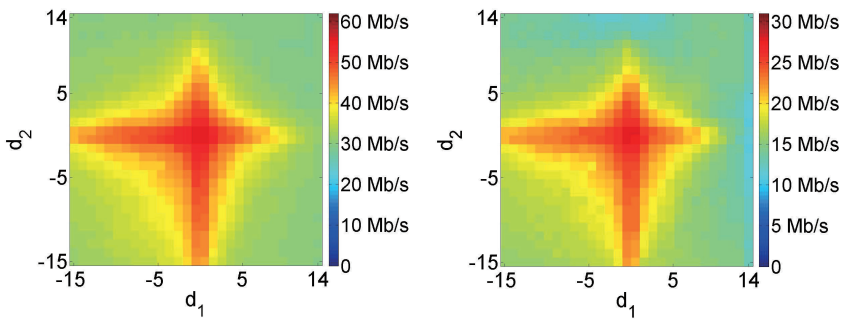

(a) Sum. throughput (b) Min. throughput

Figure 4.9: Performance of DynamicReuse.

Table 4.5: Throughput result with the residential building topology.

		Aggregate throughput	Gain over legacy
No Aggregation	Legacy	135.1 Mb/s	
	ProCCA	153.6 Mb/s	13.6%
	DynamicReuse	182.3 Mb/s	34.8%
A-MPDU	Legacy	408.7 Mb/s	
	ProCCA	442.3 Mb/s	8.2%
	DynamicReuse	504.0 Mb/s	23.3%

we conduct simulation with residential apartment topology which is proposed by TGax standard group [33]. As shown in Fig. 4.6, there is a five floor apartment building, and there are 20 apartments on each floor. In each apartment, there are a single AP and a single client station which are randomly located, and an AP operates on a randomly selected channel among three independent WLAN channels.[5] Saturated downlink UDP traffic is generated, and we conduct 100 simulations each with different deployment of WLAN nodes incuding APs and client stations and WLAN channel.

To considering the signal penetration loss due to floors and walls, we adapt a path-loss model, which is also proposed by TGax standard group [33]. Simulation parameters are summarized in Table. 4.4.

Downlink throughput of the apartments are measured and Fig. 4.10 shows the empirical CDF of the throughput result of each apartment, where the upper graph shows the result of no frame aggregation case, and the lower graph shows the result of A-MPDU case. By utilizing frame aggregation, the throughput of each scheme increases while Dy-

[5]In average sense, there are 33 APs which operate on the same channel. Accordingly, we choose 33 apartments randomly and evaluate the performance of the 33 chosen apartments for each iteration.

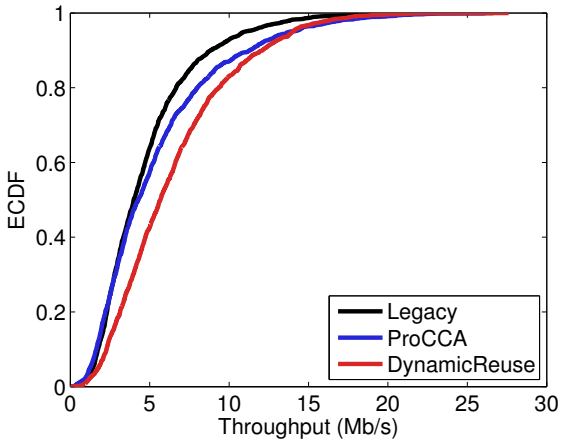

(a) No aggregation

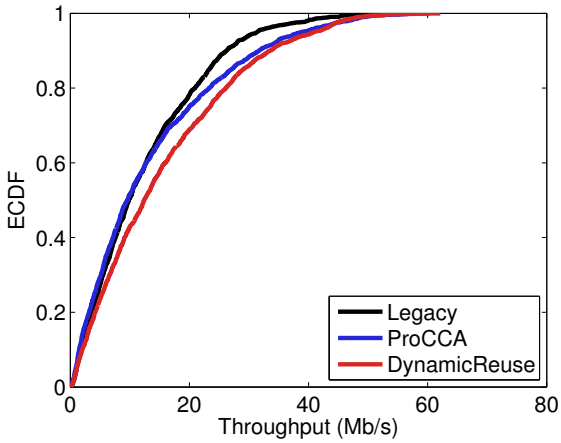

(b) A-MPDU

Figure 4.10: Empirical CDF of throughput with the residential building topology.

namicReuse outperforms others without starvation of any cell, i.e., no crossing point between ECDF curves.

The average aggregated throughput of all the apartments and the throughput gain over legacy CCA are listed in Table. 4.5. ProCCA enhances the throughput by enabling concurrent transmissions if it is feasible compared with legacy CCA, about 13.6%/8.2% for no aggregation/A-MPDU, while DynamicReuse further enhances the throughput, about 34.8%/23.3% for no aggregation/A-MPDU, via dynamic transmit power and data rate control, which increases the feasibility of concurrent transmissions.

It should be noted that the gain over legacy CCA decreases when A-MPDU is enabled, and it is mainly due to the RTS-CTS exchange and the corresponding network allocation vector (NAV) setting. After receiving RTS or CTS packet, the WLAN nodes should wait until the following data and ACK packet transmissions end, which results in a limited spatial reuse.

4.5 Summary

In this chapter, we have proposed a novel transmit power and data rate control method which dynamically control the transmit power and data rate depending on the ongoing transmission. The proposed method also adapts packet length appropriately to tackle the trade-off between spatial reuse and transmission time of data rate based on the

mathematical throughput analysis. The performance of the proposed method is evaluated via network level simulation with high density WLAN topology.

Chapter 5

Conclusion

5.1 Research Contributions

In this dissertation, we addressed MAC and PHY strategies to enhance the achievable throughput in IEEE 802.11 WLANs, and the main contributions of the dissertation are as follows.

In Chapter 2, we present an antenna subset selection system for infrastructure-based WLANs, which is applicable to commercial WLAN devices. Practical antenna selection algorithms of AP for unicast/multicast transmission and reception are proposed by considering practical issues. By alternatively using two best antenna combinations and reducing unnecessary probing overhead, the proposed algorithms achieve significant performance gain. The algorithms are evaluated via measurements with prototype implementation in a commercial AP. To the best of our knowledge, we are the first to present antenna selection

algorithms without using CSI.

In Chapter 3, we have proposed a novel CCA mechanism utilizing additional information in the PHY header to examine the feasibility of concurrent transmission. By utilizing the information in the PHY header and performing CCA depending on the ongoing transmission, ProCCA achieves spatial reuse as ideal case by solving the conservative operation of existing CCA method. Simulation results demonstrate the proposed scheme significantly enhances network throughput by promoting spatial reuse.

In Chapter 4, we have proposed a novel transmit power and data rate control method, namely DynamicReuse. DynamicReuse dynamically control the transmit power and data rate depending on the ongoing transmission so that it improves network capacity by promoting more concurrent transmissions than ProCCA. Based on the mathematical analysis, the trade-off between spatial reuse and transmission time with data rate control is tackled, and throughput loss with lowered data rate is eliminated via proper packet length adaptation of DynamicReuse. Finally, the performance of DynamicReuse is evaluated via simulation with high density WLAN environment.

To summarize, the PHY rate has increased greatly to boost the network capacity, but there are mainly two challenges to exploit the high PHY rates, namely unreliability of the high PHY rates and throughput decrease by medium sharing in high density network. By utilizing antenna subset selection, the reliability with the high PHY

rates is significantly improved to solve the reliability issue. Meanwhile, medium sharing issue is addressed and the throughput degradation is significantly reduced by achieving spatial reuse via ProCCA and DynamicReuse.

5.2 Future Research Directions

Based on the results of this dissertation, there are several new research directions which require further investigation. We highlight some of them as follows.

First, we proposed the transmit antenna selection algorithm which effectively utilizes multiple retry chains. However, the multiple retry chains are selected in a different manner for A-MPDU transmission. Specifically, only the first retry chain is used unless all the subframes of an A-MPDU fail. Accordingly, the performance of our proposed algorithm with A-MPDU should be evaluated and the algorithm should be modified if needed.

Second, the feasibility issue of ProCCA and DynamicReuse should be addressed. For the proposed two algorithm, the possibility of a concurrent transmission should be examined right after decoding PHY header, and the incoming frame can be dropped right after the decision. We only verified the performance via simulations assuming the described operation is feasible, so it should be addressed via testbed experiments.

Finally, the RTS-CTS exchange and NAV setting for A-MPDU interrupt the operations of ProCCA and DynamicReuse, which results in the limited spatial reuse. Accordingly, NAV setting for spatial reuse should be tackled to promote spatial reuse via ProCCA and DynamicReuse.

Bibliography

[1] M. Gharavi-Alkhansari and A. B. Gershman. Fast Antenna Subset Selection in MIMO Systems. *IEEE Trans. Signal Process.*, 52(2):339–347, February 2004.

[2] M. Gkizeli and G. N. Karystinos. Maximum-SNR Antenna Selection Among A Large Number of Transmit antennas. *IEEE J. Select. Topics Signal Process.*, 8(5):891–901, June 2014.

[3] A. Molisch *et al.* Capacity of MIMO Systems with Antenna Selection. In *Proc. IEEE ICC*, Helsinki, Finland, June 2001.

[4] R. W. Health and A. Paulraj. Antenna Selection for Spatial Multiplexing Systems Based on Minimum Error Rate. In *Proc. IEEE ICC*, Helsinki, Finland, June 2001.

[5] D. A. Gore and A. J. Paulraj. MIMO Antenna Subset Selection with Space-Time Coding. *IEEE Trans. Signal Process.*, 50(10):2580–2588, October 2002.

[6] H. Zhang and H. Dai. Fast Transmit Antenna Selection Algorithms for MIMO Systems with Fading Correlation. In *Proc. IEEE VTC*, Los Angeles, USA, 2004.

[7] D. Gore *et al.* Statistical Antenna Selection for Spatial Multiplexing Systems. In *Proc. IEEE ICC*, New York, USA, May 2002.

[8] D. F. Bantz *et al.*, "*Diversity Transmission Strategy in Mobile/Indoor Cellula Radio Communications*," U.S. Patent 5 507 035, Apr. 1996.

[9] W. S. Kish *et al.*, "*System and Method for Transmission Parameter Control for An Antenna Apparatus with Selectable Elements*," U.S. Patent 8 150 470 B2, Apr., 2012.

[10] J. Zhu *et al.* Leveraging spatial reuse in 802.11 mesh networks with enhanced physical carrier sensing. In *Proc. IEEE Int. Conf. Commun. (ICC)*, pages 4004–4011, June 2004.

[11] L. Fu, S. C. Liew, and J. Huang. Effective carrier sensing in CSMA networks under cumulative interference. *IEEE Trans. Mobile Comput.*, 12(4):748–760, April 2013.

[12] J. Zhu *et al.* Adaptive CSMA for scalable network capacity in high-density WLAN: A hardware prototyping approach. In *Proc. IEEE Conference on Computer Communications (INFOCOM)*, pages 1–10, April 2006.

[13] H. Ma, S. Shin, and S. Roy. Optimizing throughput with carrier sensing adaptation for IEEE 802.11 mesh networks based on loss differentiation. In *Proc. IEEE Int. Conf. Commun. (ICC)*, pages 4967–4972, June 2007.

[14] K.P Shih and Y. D. Chen. CAPC: A Collision Avoidance Power Control MAC Protocol for Wireless Ad Hoc Networks. *IEEE Commun. Lett.*, 9(9):859–861, September 2005.

[15] K. P. Shih and Y. D. Chen and C. Chang. Adaptive Range-Based Power Control for Collision Avoidance in Ad Hoc Networks. In *Proc. IEEE Int. Conf. Commun. (ICC)*, pages 3672–3677, June 2007.

[16] J. P. Monks and V. Bharghavan and W. W. Hwu. A Power Controlled Multiple Access Protocol for Wireless Packet Networks. In *Proc. IEEE Conference on Computer Communications (INFOCOM)*, pages 219–228, April 2001.

[17] S. Wu, Y. Tseng, and J. Sheu. Intelligent Medium Access for Mobile Ad Hoc Networks with Busy Tones and Power Control. *IEEE J. Select. Areas Commun.*, 18(9):1647–1657, September 2000.

[18] A. Muquattash and M. Krunz. A Single-Channel Solution for Transmit Power Control in Wireless Ad Hoc Networks. In *Proc. ACM International Symposium on Mobile Ad Hoc Networking and Computing (MobiHoc)*, pages 276–283, May 2004.

[19] Y. Eunho *et al.* An Enhanced Link Adaptation Strategy for IEEE 802.11 Wireless Ad Hoc Networks. pages 1672–1676, September 2007.

[20] C. Chen *et al.* Rate-Adaptive Framing for Interfered Wireless Networks. In *Proc. IEEE Conference on Computer Communications (INFOCOM)*, pages 219–230, May 2007.

[21] L. Zheng and D.N.C Tse. Diversity and Multiplexing: A Fundamental Tradeoff in Multiple Antenna Channels. *IEEE Trans. Inform. Theory*, 49(5):1073–1096, May 2003.

[22] A. F. Molisch and M. Z. Win. MIMO Systems with Antenna Selection - An Overview. *IEEE Microwave*, 5(1):46–56, March 2004.

[23] IEEE std. IEEE 802.11-2012, *Part 11: Wireless LAN Medium Access Control (MAC) and Physical Layer (PHY) specifications*, March 2012.

[24] IEEE std. IEEE 802.11-2013, *Part 11: Wireless LAN Medium Access Control (MAC) and Physical Layer (PHY) specifications: Enhancements for Very Higher Throughput for Operation in Bands Below 6 GHz*, December 2013.

[25] Samsung. WEA303 [Online]. Available: `http://www.samsung.com/us/business/business-communication-systems/wireless-enterprise-solutions/WDS-A303CI/XAR`.

[26] Samsung. Galaxy S3 [Online]. Available: http://www.samsung.com/global/galaxys3/specifications.html.

[27] Ixia. IxChariot 7.3. [Online]. Available: http://www.ixiacom.com/products/ixchariot.

[28] MadWiFi. Minstrel rate control. [Online]. Available: http://madwifi-project.org/browser/madwifi/trunk/ath_rate/minstrel.

[29] X. Dong and N. C. Beaulieu. Average level crossing rate and average fade duration of selection diversity. *IEEE Commun. Lett.*, 5(10):396–398, October 2001.

[30] Hanback Electronics. HBE-RoboCar. [Online]. Available: http://www.hanback.co.kr/htm/ebook/RoboraSeries.html.

[31] IEEE P802.11, *Specification Framework for TGax*, January 2016.

[32] The Network Simulator ns-3. [Online]. Available: http://www.nsnam.org/.

[33] IEEE P802.11, *TGax Simulation Scenarios*, July 2015.

[34] J. Lee *et al.* An Experimental Study on the Capture Effect in 802.11a Networks. In *Proc. ACM WiNTECH*, September 2007.

[35] Daji Qiao, Sunghyun Choi, and Kang G. Shin. Goodput analysis and link adaptation for IEEE 802.11a wireless LANs. *IEEE Trans. Mobile Comput.*, 1(4):278–292, October 2002.

초 록

IEEE 802.11 기반의 무선랜 기술은 꾸준한 발전을 통해 현재 많은 디바이스들에 이용되고 있으며, 세계적 chipset 출하량 및 mobile data traffic량 역시 꾸준히 증가하고 있다, 이런 무선랜의 성능을 향상시키기 위해서 대표적으로 2009년 802.11n, 2013년 802.11ac 표준이 정의 되었으며, 이들 표준에서는 throughput 향상을 위해 physical layer (PHY) rate을 높이는 것과 MAC efficiency를 높이는 것에 중점을 두고 있다, 특히, PHY rate을 높이기 위해서 multiple stream 동시전송, channel bonding, 256QAM 등을 적용하였으며, 802.11ac 표준을 이용하면 1 Gb/s이 넘은 PHY rate을 사용할 수 있다. 하지만 높은 PHY rate으로 갈수록 reliability가 떨어져서 coverage가 감소하는 문제가 있으며, 높은 PHY rate을 쓰더라도 노드가 많이 밀집된 환경에서는 throughput이 감소하는 문제가 있다.

이러한 문제들은 해결하기 위해 본 학위논문에서는 다음과 같은 세 가지 연구를 담고 있다. 첫째로, 높은 PHY rate에서도 reliability를 향상시키기 위해 antenna subset selection이라는 기술을 도입하고, 현실적인 이슈들을 고려하여 실재 디바이스에서 동작하는 알고리즘을 고안하였다. 둘째로, 노드가 많이 밀집된 환경에서도 spatial reuse를 통해 throughput을 향상시키기 위한 carrier sensing 기법에 대한 연구를 진행하였다. 기존 clear channel assessment (CCA)의 한계를 극복하기 위해 PHY header 정보를 이용하여 동시전송이 가능하면 최대한 spatial reuse를 활용하는 새로운 CCA 기법을 고안하였다. 마지막으로, 동시 전송을 하는 경우, 전송 전력을 낮춰 간섭을 줄이고 전송률을 낮춰 reliability를 향상시키는 방법을 통해 동시전송의 가능성을 높여, spatial reuse를 더욱 확장시킬 수

있는 기법을 고안하였다.

제안한 세 가지 방법들은 실재 디바이스를 이용한 실측이나 네트워크 시뮬레이션을 통하여 성능이 검증되었으며, 무선랜의 효율을 크게 향상시킬 것으로 기대된다.

주요어 : Wireless LAN (WiFi), **안테나 선택, 공간 재사용**
학번 : 2011-30245